

Optimization of machining parameters of Nomex honeycomb
core for the development of a mesoscale numerical model to
predict deformation and failure in core structures



Author

Hassan Habib

Regn Number

318003

Supervisor

Dr. Muhammad Salman Khan

DESIGN AND MANUFACTURING ENGINEERING
SCHOOL OF MECHANICAL & MANUFACTURING ENGINEERING
NATIONAL UNIVERSITY OF SCIENCES AND TECHNOLOGY
ISLAMABAD
AUGUST, 2023

Optimization of machining parameters of Nomex honeycomb
core for the development of a mesoscale numerical model to
predict deformation and failure in core structures

Author

Hassan Habib

Regn Number

318003

A thesis submitted in partial fulfillment of the requirements for the degree of
MS Design & Manufacturing Engineering

Thesis Supervisor:

Dr. Muhammad Salman Khan

Thesis Supervisor's Signature: _____



DESIGN AND MANUFACTURING ENGINEERING
SCHOOL OF MECHANICAL & MANUFACTURING ENGINEERING
NATIONAL UNIVERSITY OF SCIENCES AND TECHNOLOGY,
ISLAMABAD
AUGUST, 2023

Thesis Acceptance Certificate

Certified that final copy of MS/MPhil Thesis Written by Mr. Hassan Habib (Registration No: 00000318003), of School of Mechanical and Manufacturing Engineering (School/College/Institute) has been vetted by undersigned, found complete in all respects as per NUST Statutes/ Regulations, is free of plagiarism, errors and mistakes and is accepted as partial fulfillment for award of MS/MPhil Degree. It is further certified that necessary amendments as pointed out by GEC members of the scholar have also been incorporated in the said thesis.

Signature: _____



Name of the supervisor: Dr. Muhammad Salman Khan

Date: 24/8/2023

Signature (HOD): _____



Date: _____


24-08-23

National University of Sciences & Technology
MASTER THESIS WORK

We hereby recommend that the dissertation prepared under our supervision by: (Student Name & Regn No.) Hassan Habib (318003)
 Titled: Optimization of machining parameters of Nomex honeycomb core for the development of a mesoscale numerical model to predict deformation and failure in core structures be accepted in partial fulfillment of the requirements for the award of MS Design and Manufacturing Engineering degree.

Examination Committee Members

1. Name: Dr. Shahid Ikramullah Butt Signature: 
2. Name: Dr. Syed Hussain Imran Signature: 
3. Name: Dr. Adnan Munir Signature: 

Supervisor's name: Dr. M. Salman Khan Signature: 
 Date: 24/8/2023


 Head of Department

24/8/2023
 Date

COUNTERSIGNED

Date: 24-08-23


 ↓ Dean/Principal

Declaration

I certify that this research work titled "*Optimization of machining parameters of Nomex honeycomb core for the development of a mesoscale numerical model to predict deformation and failure in core structures*" is my own work. The work has not been presented elsewhere for assessment. The material that has been used from other sources it has been properly acknowledged / referred.



Signature of Student

Hassan Habib

2019-NUST-MS-DME-318003

Plagiarism Certificate (Turnitin Report)

This thesis has been checked for Plagiarism. Turnitin report endorsed by Supervisor is attached.



Signature of Student

Hassan Habib

Registration Number

318003



Signature of Supervisor

Copyright Statement

- Copyright in text of this thesis rests with the student author. Copies (by any process) either in full, or of extracts, may be made only in accordance with instructions given by the author and lodged in the Library of NUST School of Mechanical & Manufacturing Engineering (SMME). Details may be obtained by the Librarian. This page must form part of any such copies made. Further copies (by any process) may not be made without the permission (in writing) of the author.
- The ownership of any intellectual property rights which may be described in this thesis is vested in NUST School of Mechanical & Manufacturing Engineering, subject to any prior agreement to the contrary, and may not be made available for use by third parties without the written permission of the SMME, which will prescribe the terms and conditions of any such agreement.
- Further information on the conditions under which disclosures and exploitation may take place is available from the Library of NUST School of Mechanical & Manufacturing Engineering, Islamabad.

Acknowledgements

Allah's will is the energy that powers up this world and makes things possible. First and foremost, I am thankful to Allah for His grace due to which I was able to complete my thesis in MS in Design and Manufacturing Engineering. I am thankful to my parents whose desire of excellence has led me to believe in myself and pursue my dreams and better myself both academically and personally. I am thankful to my sister who has always been on my side and has helped me through thick and thin. I am tremendously thankful to my wife and kids for their constant and unwavering support and for their motivation to finish what I have started.

I am profusely thankful to my advisor Dr. Muhammad Salman Khan for his support and guidance throughout my thesis. His concern for my thesis and his interest really kept me going and through his inspiration I have been able to achieve this milestone. I am thankful to Mr. Danyal for the warm support and guidance he offered. Mr. Waseem and Haji sahb the staff of SMME were also very supportive and helped me in the experimentation phase. I am thankful to Mr. Adnan Munir whose support led us to do the experimentation on Honeycomb core. I am thankful to Mr. Muhammad Abdullah and Noor Hassan for their support without which it would not have been possible to do all the tasks necessary for this dissertation. I am thankful to @Vitarka @abaqus tutorials YouTube channels for their guidance in learning the statistical analysis tools and simulation in abaqus. Last but not the least I am thankful to my dear friend Mr. Muzzamil Tariq for his support in my simulations, his valuable input made it possible to complete my thesis. I am thankful to all the people who have been associated with me and have helped me directly or indirectly to complete this thesis work.

This work is dedicated to love of knowledge, independent enquiry and the thirst of excellence which has always led humanity to achieve the unthinkable and unimaginable.

Abstract

Nomex ® Honeycomb core is the foundational building block for the manufacturing of aerospace composite components. Its usage requires machining honeycomb in complex aerodynamic profiles which is of prime importance because of the complexities of the geometry involved. Machining defects of honeycomb core may result in the failure of sandwich structures when subjected to impact failures or fatigue failures. The quality of Honeycomb Core (HC Core) is governed by the accuracy and precision of these cut profiles. The assessment of accuracy and precision is directly related to the forces induced in the cutting tool and the cutting efficiency. These two parameters form the basis of a multi objective function that this paper aims to optimize for the milling operation. Based on literature review spindle speed, feed rate and depth of cut are taken as the influencing parameters. Taguchi based array of Design of Experiments is used to construct the experiments followed by ANOVA analysis and correlation analysis. The results indicate that the most significant factor is the feed rate with percentage contribution of 72% for the cutting forces and depth of cut with percentage contribution of 85% in case of cutting efficiency. The two parameters are then optimized using Desirability Function Analysis (DFA) and Grey Relational Analysis (GRA). The results are validated by experimental runs and the error is within 5% of the statistical predictions, whereas the percentage improvement in cutting forces for optimum run as compared to worst experimental run is 47.8%. The percentage improvement in cutting efficiency likewise is 11%. Numerical model was built on ABAQUS to simulate the machining process and the simulation was run using 2D Hashin Criteria. Furthermore, the simulation of the Honeycomb core was done using Johnson Cook Criteria.

Key Words: *Nomex Honeycomb Core Machining, Multi-Objective Optimization, Grey Relational Analysis, Desirability Function Analysis, ANOVA, ABAQUS Simulation.*

Table of Contents

Thesis Acceptance	iv
Declaration	v
Plagiarism	vi
Copyright Statement	vii
Acknowledgements	viii
Abstract	x
Table of Contents	xi
List of Figures	xiii
List of Tables	xiv
CHAPTER 1: INTRODUCTION	1
1.1 Background, Scope and Motivation	1
1.2 Honeycomb Structures	2
1.3 Types of Honeycomb	2
1.4 Geometry of honeycomb cores	3
1.5 Processing of Honeycomb Cores	5
1.6 Optimization of machining process.....	7
1.7 Simulation of Honeycomb core machining	10
1.8 Literature Review Summary and Research Gap	11
Chapter 2: Methodology	14
2.1 Process flow of research.....	14
2.2 Experimentation	15
2.2.1 Tool, Workpiece, and machine	15
2.2.2 Machining Fixture	17
2.2.3 DoE parameters for machining	17
2.2.4 Response Variables and Measurements	19
2.3 Data Analytics and Optimization	20
2.3.1 Desirability Function Analysis	21
2.3.2 Grey Relational Analysis	23
2.3.3 Prediction and validation of results.....	24
2.4 Simulation and damage model development.....	25
Chapter 3: Results and Discussion	27
3.1 Experimental results.....	27
3.2 Data Analytics	27
3.3 Multi-Objective Optimization	31
3.3.1 Desirability Function Analysis (DFA).....	31
3.3.2 Grey Relational Analysis	32

3.4	Conclusion	35
Chapter 4: Simulation of Machining Honeycomb cores		37
4.1	Process of simulation	37
4.2	Simulation of simple machining process.....	38
4.3	Evaluation of Hashin Damage Criteria	39
4.4	Simulation of Nomex Honeycomb Core	43
Chapter 5: Conclusions and Recommendations		45
5.1	Conclusions.....	45
5.2	Future Recommendations.....	46
REFERENCES		48
APPENDIX A.....		52
VISUAL RESULTS OF EXPERIMENTS		52

List of Figures

Figure 1 Shear Strength for different directions of 5052 aluminum honeycomb (Ko & Wu, 1998).	3
Figure 2 Various types of cell chapes	4
Figure 3 Various elements of honeycomb geometry	5
Figure 4 (a) Machining of Honeycomb Cores. (b) Ultrasonic Machining of HC Core.	6
Figure 5 Ice Freezing method for machining of HC Cores	6
Figure 6 (a) Burr Formation (Jaafar, Makich, et al., 2021) (b) Delamination and tearing of wall (Zarrouk, Salhi, Nouari, et al., 2021)	7
Figure 7 (a) Mesomodel (b) Homogeized Model (c) Shell Model (Jaafar, Nouari, et al., 2021)	10
Figure 8 Nomex® paper modelling approaches. a) Isotropic monolayer; b) orthotropic monolayer; c) multilayer; d) multilayer with resin at the junctions.....	11
Figure 9 Summary of Literature Review	12
Figure 10 Methodology of Research.....	14
Figure 11 Nomex Honeycomb Core Block.....	15
Figure 12 Cutting Tool Nomenclature	16
Figure 13 CNC Machine of YDPM	16
Figure 14 (a) Isometric view of Fixture Plate; (b) Front view of fixture plate; (c) Actual Experimental Setup	17
Figure 15 Trial Run Results for Forces in X-Axis.....	19
Figure 16 Keyence Image Dimensional Measurement System	20
Figure 17 Measurements from Keyence system	20
Figure 18 Steps for Taguchi Analysis.....	21
Figure 19 Steps for ANOVA Analysis	21
Figure 20 Steps for Desirability Function Analysis	22
Figure 21 Steps for GRA	23
Figure 22 Feed Rate vs Force (F) vs Spindle Speed	28
Figure 23 Feed Rate vs Cutting Efficiency vs Depth of Cut.....	28
Figure 24 Main Effects Plot for S/N ratios (a) Force & (b) CE.....	30
Figure 25 Results of Grey Relational Analysis.....	32
Figure 26 Top cut represents run 7 (best run) bottom cut represents run 6 (worst run).....	33
Figure 27 Comparison of predicted, validated and worst runs	35
Figure 28 CAD Model of cutting tool.....	39
Figure 29 Simulation of Machining Process.....	40
Figure 30 Simulation of 2D shell composite element using Hashin Damage Criteria.....	40
Figure 31 Results of Simulation	41
Figure 32 3D stresses during machining.....	42
Figure 33 (a) Encastrate Constraint for workpiece (b) Rigid Body for tool	43
Figure 34 Meshing of Honeycomb Core	44
Figure 35 Simulation Results.....	44
Figure 36 Experiment # 4, 5, 6	52
Figure 37 Experiment # 1, 2, 3	52
Figure 38 Experiment # 7, 8, 9	53

List of Tables

Table 1 Literature Review of Cutting Parameters in different research works	7
Table 2 Geometrical Properties of Nomex Honeycomb Core.....	15
Table 3 Specifications of Cutting Tool	16
Table 4 Taguchi Design of Experiments.....	18
Table 5 Parameters for DoE.....	18
Table 6 Experimental Results	27
Table 7 Response Table for SN Ratios (Force).....	29
Table 8 Response Table for SN Ratios (CE).....	29
Table 9 ANOVA Table of S/N ratios for F.....	29
Table 10 ANOVA Table for S/N ratios for CE.....	29
Table 11 Percentage Contribution based on ANOVA	29
Table 12 Response Optimization through Composite Desirability Function	32
Table 13 Response Table for GRG	33
Table 14 Optimum Levels based on GRG & DFA	33
Table 15 Predicted results from ANOVA	34
Table 16 Validation Results	34
Table 17 Johnson Cook Material Properties for plasticity	39
Table 18 Constants for damage model based on the Johnson Cook Criteria	39

CHAPTER 1: INTRODUCTION

The research work in this dissertation has been presented in a total of six parts. First part is related to the introduction of the topic. It elaborates the criticality of the current research in terms of its application in the aerospace industry, literature review, gaps in the concerned area of research and the novelty that is offered through this research. Second part outlines the methodology adopted and elaborates the tasks outlined in this dissertation. Third part concerns itself with the experimentation phase of the current research and considers the data analytics used to describe and optimize the results of the machining process of Honeycomb core. Fourth part elaborates the laborious analysis conducted in ABAQUS to simulate the machining process of Nomex Honeycomb Core. The fifth part concludes the research by outlining the outcomes of this dissertation and recommends some prospects that could be undertaken in this area of research.

1.1 Background, Scope and Motivation

Aerospace sector extensively relies on honeycomb core based raw materials for the manufacturing of aircrafts (Aerospace Engineering and Operations Technician, Bureau of Labor Statistics, U.S. Department of Labor, n.d.). The aerostructures are heavily profiled to cater for the aerodynamic stability of the structures. With advancements in technology lightweight, energy efficient, and robust materials are used for aircraft manufacturing. In this arena of new materials honeycomb cores stand out because of their extraordinary out-of-plane compressive and shear strengths (Heimbs, 2009b)(Liu et al., 2015). Some of the examples of aircraft components made from honeycomb cores are fairings, rudders, overhead stowage bins etc. Manufacturing of these aircraft structures requires machining of honeycomb cores to mold them into the final product by subsequent addition of composite layers. It is viable to produce good quality sandwich structures only when the machining process induces the least defects in the cut honeycomb. The cutting process is chip extensive and due to delamination; it is necessary to find out the cutting efficiency of the process as well, which has not been considered in the literature up till now. This forms an important part for the present research as multi objective optimization is performed to determine the most critical factors that affect the cutting forces and the cutting efficiency. It is also possible to predict the behavior of cores by using simulation (Zarrouk, Nouari, et al., 2022). For this damage model based on Hashin Criteria is mostly used in the literature (Hashin, 1980). The simulation

results validate the experimental results.

The following chapter provides a literature review on the honeycomb core structures, its properties, its applications, manufacturing of honeycomb cores, defects encountered during machining, simulation studies conducted on honeycomb cores and finally the research gap identified in the literature for out current research.

1.2 Honeycomb Structures

Various types of honeycombs are widely used, and they encompass a range of materials such as uncoated and resin-infused kraft paper, diverse aluminum alloys, aramid paper, and glass or carbon fiber-reinforced plastics with different fabric weaves and resin systems. While honeycombs based on titanium, stainless steel, and other materials see less frequent use, they still play essential roles.

Honeycomb cores are typically constructed by bonding thin material strips together using adhesive. Aramid paper honeycomb stands out due to its inherent toughness and resistance to abuse. Cores with densities ranging from 16 to 48 kg/m³ (1 to 3 lb/ft³) are excellent choices for applications such as aircraft cabin interior walls and ceilings. These cores can even be paired with glass fabric-reinforced skins as thin as 0.254 mm (HEXCEL, 2015).

The physical and mechanical properties of honeycomb core materials are strongly dependent on the properties of the base materials used in their manufacturing. However, it's essential to note that several key properties of honeycomb cores are specific to the materials employed and should be considered separately (Ko & Wu, 1998).

1.3 Types of Honeycomb

There are various types of honeycomb cores available in the market and their use varies according to the area of their application. Commonly used materials (Ko & Wu, 1998) in honeycomb cores are:

- Paper Honeycomb
- Aluminum Honeycomb
- Glass fiber reinforced plastic honeycomb
- Aramid paper honeycomb
- Reinforced plastic honeycomb
- Kevlar honeycomb
- Kevlar paper honeycomb

The honeycomb core used in the construction of sandwich materials is composed of various materials and grades (Zenkert, 1995). The most common material is phenolic resin impregnated aramid fiber know as Nomex® (*Honeycomb Composite*, n.d.). It is most commonly used because it's flame retardant, provides better insulation and has good dielectric properties (Liu et al., 2015).

1.4 Geometry of honeycomb cores

The quality of the manufactured sandwich structures largely depend on the quality of the machining process and properties of the honeycomb material (Jaafar, Makich, et al., 2021). A lot of research has been conducted to probe into the properties of honeycomb cores and today the complete material characterization of standard Nomex core is available in the literature (Zinno et al., 2011)(Chiang Foo et al., 2006). The characterization of properties largely depend on the thickness of side walls and the length of sides of honeycomb structure (Hu & Yu, 2010). Other geometrical properties of honeycomb include cell size, cell thickness, angle between two adjacent sides and the shape of core structure. These geometrical properties influence the material properties of honeycomb cores greatly. Some of the important properties are discussed below:

- Cell Shape and Anisotropy

Honeycomb structures exhibit anisotropy, resulting in directional properties tailored to anticipated loads. Figure 1 illustrates variations in shear strength along the L and W directions. Some cell shapes permit easy shaping or curving with minimal sacrifice in the strength-to-weight ratio. This feature holds significant value in the fabrication of curved components with substantial thickness.

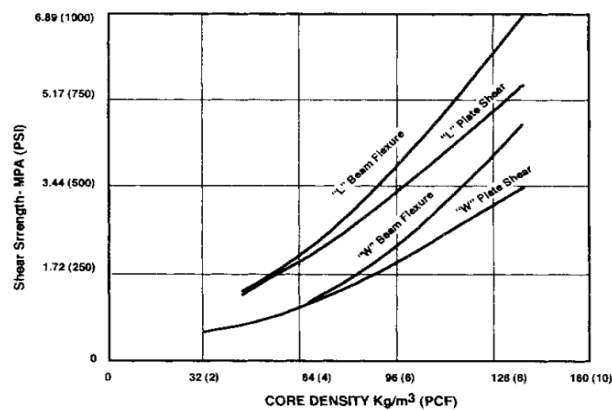


Figure 1 Shear Strength for different directions of 5052 aluminum honeycomb (Ko & Wu, 1998).

- Variations in Cell Shape

Modifications in cell shape can be either specified by the core manufacturer or

unintentionally altered by the user, particularly in materials like aluminum. It's important to note that under- or over-expanding the core changes its cell shape and density. Over-expanding, as depicted in Fig. 2 alters directional properties, potentially making the L direction slightly weaker of the two major axes. This can result in up to a 30% reduction in L direction strength, underscoring the need to prevent inadvertent changes in cell shape.

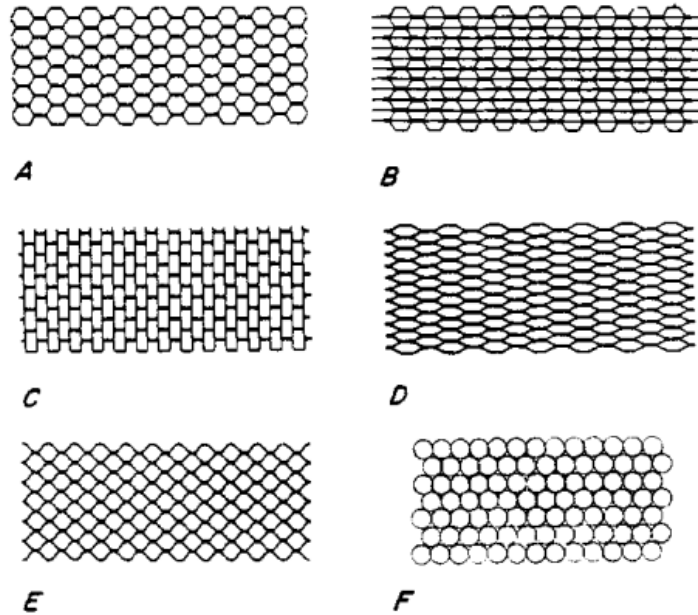


Figure 2 Various types of cell chapes

- **Cell Size Impact**

While cell size is typically a secondary consideration for most core material mechanical properties, it plays a primary role in determining the strength of the core-to-face attachment. It also affects the stress levels at which intracell buckling or facings' dimpling occurs.

- **Thickness Considerations**

To accurately assess shear and compressive properties of a specific core type, precise test methods and controlled thickness must be used. Neglecting the thickness factor can lead to observed values being off by a factor of 4 or more (Ko & Wu, 1998).

Various elements of geometry of honeycomb cells are depicted in Fig. 3.

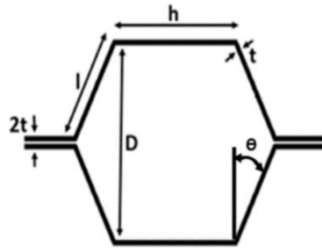


Figure 3 Various elements of honeycomb geometry

1.5 Processing of Honeycomb Cores

The biggest challenge in manufacturing parts through honeycomb core is their transformability. There are very less shapes available that could be directly used to manufacture the end products (HEXCEL, 2015) and thus, it is inevitable that the honeycomb cores would be subject to forming processes. Among many processes the most used process to shape honeycomb cores is the machining process. This process is usually performed using machine tool (Jaafar et al., 2017) Fig.4 (a) or the ultrasonic energy using abrasives (Ahmad et al., 2020) Fig.4 (b). Some of the researchers have proposed special setups (low temperature fixtures) for the machining process for the reduction of machining defects (Qiu et al., 2017) Fig.5. Others have proposed cutting honeycomb core by using special multi helix cutting tools with chip breakers (Jaafar, Nouari, et al., 2021). However, in literature the cutting efficiency of the process in terms of cut width and actual tool diameter has not been evaluated along with cutting forces.

The main defects that occur during machining of honeycomb cores are crushing, chipping, fraying, tearing, and surface deformation (Liu et al., 2015) (Zarrouk et al., 2023). These defects influence the quality of the sandwich structure that is subsequently produced using the core material. The poor quality of machined surface directly influences the formation of sandwich materials when the adhesive layer or meniscus is inserted between the composite lamination layer and honeycomb core. The literature suggests that the amount of meniscus (adhesive layer) between the composite lamination layer and core material should not be less than 300 μm (Rion et al., 2008). The machining defects greater than this could cause irregularities in the formation of sandwich panels resulting in the loss of desired mechanical properties. These defects also decrease the cutting efficiency of the process which is critical to achieve close tolerances in aerospace structures. Yongqing (et. al) have studied the surface roughness through 3D surface roughness

measurement system and have concluded that roughness of $218 \mu\text{m}$ can be achieved through process optimization (Y. Wang et al., 2020).

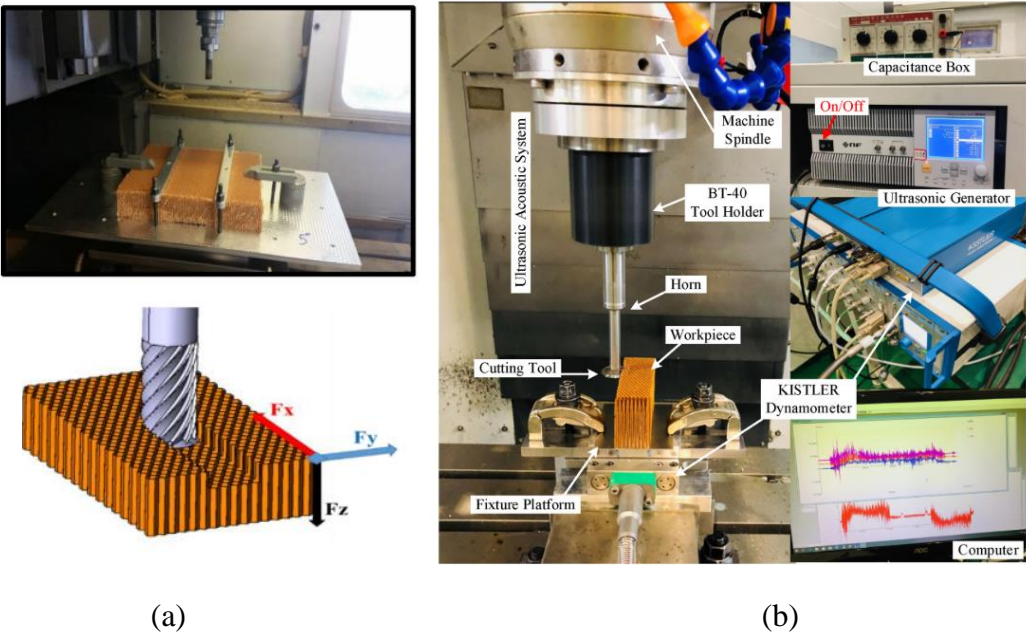


Figure 4 (a) Machining of Honeycomb Cores. (b) Ultrasonic Machining of HC Core.

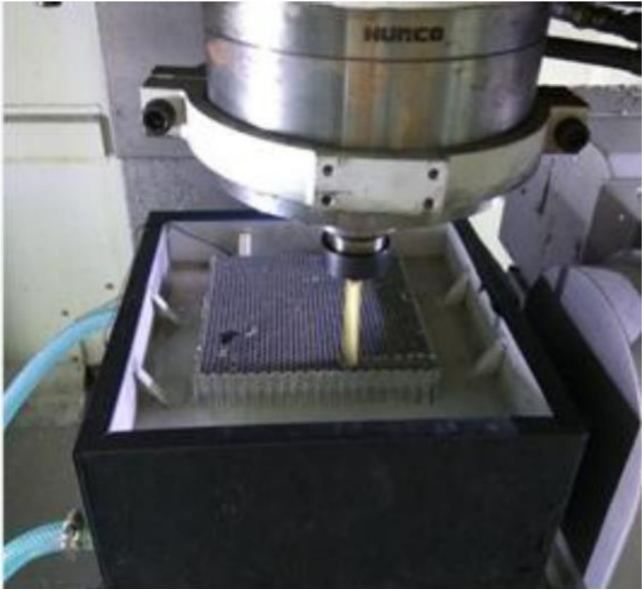


Figure 5 Ice Freezing method for machining of HC Cores



Figure 6 (a) Burr Formation (Jaafar, Makich, et al., 2021) (b) Delamination and tearing of wall (Zarrouk, Salhi, Nouari, et al., 2021)

1.6 Optimization of machining process

Owing to these challenges researchers have tried to optimize the machining process of honeycomb cores and composite materials (Y. Wang et al., 2020)(Jenarathanan & Jeyapaul, 2018)(Zarrouk, Nouari, et al., 2022). Various parameters related to machining were analyzed in the literature. M. Jaafar (Jaafar et al., 2017) has performed the experimentation of the machining process and concluded that the most significant factor during machining is the feed rate (Jaafar, Makich, et al., 2021). Similarly, others have conducted only the simulated studies and have concluded that the simulation is consistent with the experimental results (Zarrouk, Salhi, Atlati, et al., 2021). The considered factors by these authors were feed rate, spindle speed and depth of cut while the response variables were mainly forces. Various factors studied by different authors for machining of composite materials are summarized in Table 1.

Table 1 Literature Review of Cutting Parameters in different research works

Sr. #	RP Title	Material Type	Cutting Parameters	Levels	Optimization
1.	Study on the cutting force in machining of aluminum honeycomb core material. Kunxian Qiu (2016) (Qiu et al., 2017)	Al Honeycomb core	<ul style="list-style-type: none"> i. Rake Angle ii. Clearance Anlge iii. Axial Rake Angle iv. Entrance Angle v. Cutting Speed vi. Cutting Depth vii. Cutting Width 	<ul style="list-style-type: none"> i. 75, 60, 45, 30, 15 ii. 5 ii. 60, 45, 30 iv. 1, 15, 30, 45, 60, 75, 90, 105, 120, 135, 150, 165, 179 v. 240 m/min vi. 1 	ANOVA

				vii. 0.2, 0.1, 0.05	
2.	A study on milling of glass fiber reinforced plastics manufactured by hand-lay up using statistical analysis (ANOVA). J. Paulo Davim (2004) (Davim et al., 2004)	GFRP	i. Cutting Velocity ii. Feed Rate iii. Spindle Speed	i. 47, 79, 110 m/min ii. 0.04, 0.08, 0.12 (mm/rev) iii. 3000, 5000, 7000	ANOVA
3.	An experimental investigation into the orthogonal cutting of unidirectional fibre reinforced plastics. X.M Wang (2003) (X. M. Wang & Zhang, 2003)	FRP	i. Cutting Speed ii. Fibre Orientation iii. Rake Angle iv. Depth of Cut	i. 1 m / min ii. 0, 30, 60, 90, 120, 150 iii. -20, 0, 20, 40 iv. 0.001, 0.05, 0.1	Direct Correlation
4.	Modeling and numerical simulation of the chip formation process when machining Nomex. Tarik (2021)(Zarrouk, Salhi, et al., 2022)	Nomex Honeycomb	i. Feed Rate ii. Spindle Speed iii. Depth of cut	i. 200, 1000, 3000 (mm/min) ii. 5000, 10000, 15000, 23000 iii. 2 mm	ABAQUS EXPLICIT
5.	A 3D FE modeling of machining process of Nomex® honeycomb core: influence of the cell structure behaviour and specific tool geometry. (2017) Jaafar (Jaafar et al., 2017)	Nomex Honeycomb	i. Feed Rate ii. Spindle Speed	i. 200, 3000 (mm/min) ii. 2000, 15000, 23000	Comparison on ABAQUS
6.	Optimisation of machining parameters on milling of GFRP composites by desirability function analysis using Taguchi method. M.P Jenarathanan (2018) (Jenarathanan & Jeyapaul, 2018)	GFRP	i. Fibre Orientation Angle ii. Helix Angle iii. Spindle Speed iv. Feed Rate (mm/rev)	i. 15, 60, 105 ii. 25, 35, 45 iii. 2000, 4000, 6000 iv. 0.04, 0.08, 0.12	Desirability Function Analysis based on Taguchi Method
7.	3D numerical modeling and experimental validation of machining Nomex® honeycomb	Nomex HC	i. Feed Rate ii. Spindle Speed	i. 200, 1000, 1500, 3000 ii. 2000, 10000, 15000, 23000	ABAQUS Simulations

	materials. Jaafar (2021) (Jaafar, Nouari, et al., 2021)				
8.	Study of the surface defects and dust generated during trimming of CFRP: Influence of tool geometry, machining parameters and cutting speed range. Madjid (2014) (Haddad et al., 2014)	CFRP	i. Feed Rate ii. Cutting Speed iii. Depth of cut	i. 500, 1000, 15000 ii. 150, 250	ANOVA Analysis, SEM Images

Similar studies have been conducted for Fiber Reinforced Plastics (FRPs). (Jenarthanan & Jeyapaul, 2018) has optimized the machining process of Glass FRPs using composite desirability function while considering helix angle of tool, fiber orientation angle, spindle speed and feed rate. The author has examined the effect of these variables on cutting force and delamination factor. Similar studies were conducted by (X. M. Wang & Zhang, 2003) (Davim et al., 2004) and (Haddad et al., 2014). These authors have used ANOVA, correlation methods, and SEM image-based methods to optimize the machining process of different FRPs, however, only (Jenarthanan & Jeyapaul, 2018) has considered a variable of delamination factor that is similar to the cutting efficiency considered in the present research. (Jenarthanan & Jeyapaul, 2018) proposed the delamination factor as a response variable for machining of FRPs, however, this factor, has not been studied for honeycomb core-based structures.

Aluminum honeycomb cores are also widely used in aerospace and automotive sectors and (Qiu et al., 2017) has conducted research on milling process efficiency of aluminum honeycomb core. Simulation on DEFORM was used to determine the most significant contribution factors while taking rake angle, clearance angle. Cutting speed, depth of cut, width of cut and axial rake angle as input parameters. The response variable was cutting force. (Makich et al., 2022) has also analyzed machining of aluminum honeycomb cores and while considering feed rate and spindle speed as the factors and force as the response variable. The authors have devised an image processing protocol to assess the quality of machined surface for burr formation. The authors have not considered the effects of depth of the cut on the quality of the cut honeycomb cores.

1.7 Simulation of Honeycomb core machining

The simulation of honeycomb cores has been studied widely by authors (Chiang Foo et al., 2006). Broadly three approaches are used by the scientists for the honeycomb core: a) meso-models b) homogenized models c) shell models. Maximum information about failure is provided by the meso-models followed by homogenized models and shell models (Heimbs, 2009a) (Seemann & Krause, 2017). However, computational time for meso-models is high owing to a large number of analysis points (Z. Wang et al., 2017). Furthermore, the modelling of Nomex® is performed using multiple methodologies (Seemann & Krause, 2017) including a) single layer isotropic b) single layer orthotropic c) multilayer resin coat d) multilayer resin corner Fig.7.

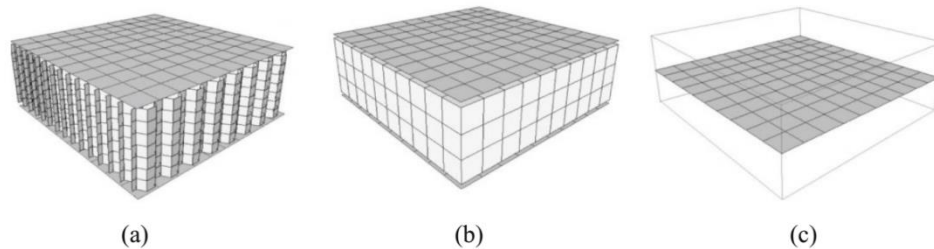


Figure 7 (a) Mesomodel (b) Homogeized Model (c) Shell Model (Jaafar, Nouari, et al., 2021)

The modelling of properties of Honeycomb cores also require different approaches and the most important ones are elaborated here for reference. 1) Assign isotropic behavior at the walls of the honeycomb with an elastic-plastic properties. It is easy to setup however, it neglects the composite architecture of the Nomex paper. 2) Represent a single layer orthotropic Nomex paper modelling which represents more possibilities of Nomex paper modelling. 3) In third approach, Nomex® paper is modelled using a multi-layer structure by the representation of three layers with an isotropic behaviour for phenolic resin coating, two layers of this resin envelope the aramid paper, this latter can be modelled as an isotropic or orthotropic material. (4) Lastly, Nomex® paper is modelled using a multi-layer structure with the addition of the resin accumulation in the hexagon corners of the cells. All these studies treat the mechanical behaviour of honeycomb structures under mechanical stress such as out-of-plane compression, shear and impact loading (Zarrouk et al., 2023). The graphics of these modelling properties are shown in Fig 8.

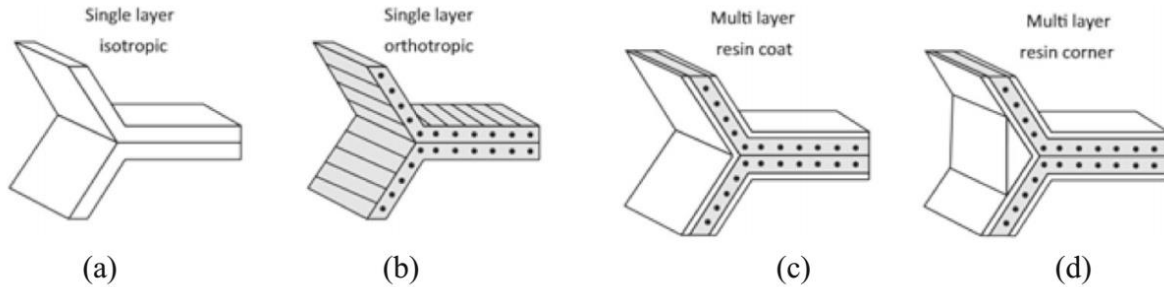


Figure 8 Nomex® paper modelling approaches. a) Isotropic monolayer; b) orthotropic monolayer; c) multilayer; d) multilayer with resin at the junctions

The damage mechanics-based models are utilized to predict the failure of honeycomb cores. These models rely on the approach adopted to model the core. Among these models the most popular are the Hashin, Tsai-Wu, Tsai-Hill, and Johnson Cook criterion. Damage evolution in case of material stiffness is studied through Johnson Cook method by (Sun et al., 2020). The Tsai-Wu criterion is an interactive criterion that extends the Von Mises criterion to account for isotropic materials in a generalized manner (Padhi et al., 1997). The Tsai-Hill criterion is typically employed at the lamina level and characterizes a failure envelope with a smooth elliptical shape. To incorporate stress and strength interactions in both the fiber and matrix directions, the Tsai-Hill criterion has been expanded and generalized, resulting in the development of the Tsai-Wu criterion (C. H. Wang & Duong, 2016). While Tsai-Wu criteria identifies damage of each element the Hashin criteria enables to identify the further modes and directions of the failure (Hashin, 1980).

1.8 Literature Review Summary and Research Gap

The extensive literature review carried out was summarized in the foregone chapter and the summary of the same is appended below for reference. The literature review has demonstrated the importance of cutting honeycomb and highlighted the major techniques that are utilized for the said purpose. It also highlights the machining practices of other composite materials such as Glass Fiber Reinforced Plastics, and Carbon Reinforced Plastics. The summary of this literature review is shown in Fig. 9. The problem statement extracted from the review is machining of Honeycomb is extensively used to cut profiled surfaces for subsequent manufacturing of Aerospace parts. This process is immune to various defects including burr formation, fraying, tearing and delamination. These defects degrade the quality of sandwich structures built through honeycomb cores. These

defects are influenced by cutting forces and cutting efficiency. Therefore, it is necessary that the process is optimized vis-à-vis these prime influencing factors.

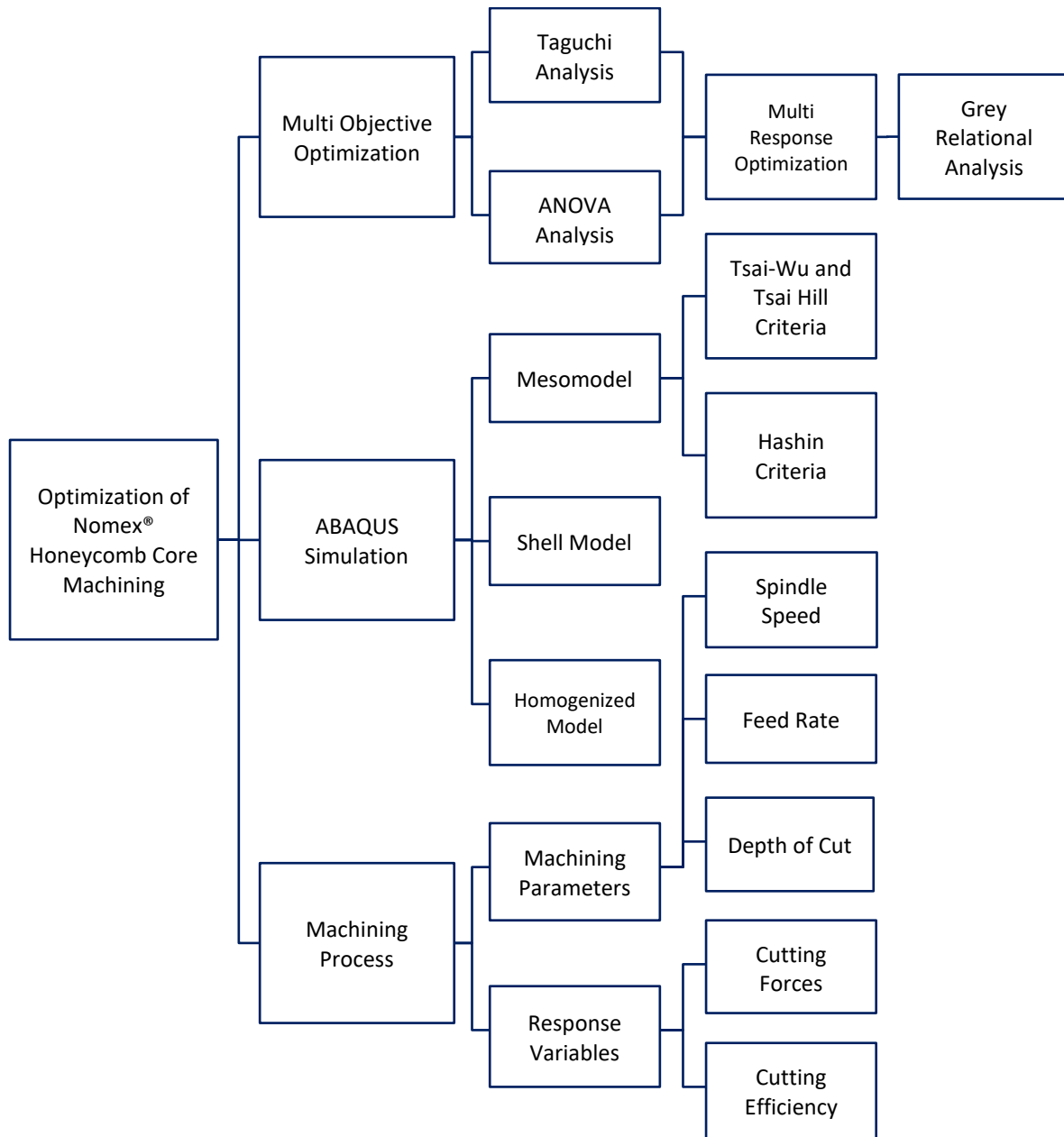


Figure 9 Summary of Literature Review

Foregone, the present study considers the optimization of machining process of Nomex® honeycomb cores through multi-objective optimization techniques of Desirability Function Analysis (DFA) and Grey Relational Analysis (GRA). The considered factors are spindle speed, feed rate and depth of cut. The response factors considered are force and cutting efficiency. Firstly,

Taguchi L9 array is used to construct experimental runs. Secondly, Taguchi analysis and ANOVA is performed to establish the most significant factors for the machining process. Thirdly, optimization using DFA and GRA is performed. Fourthly, validation runs are executed to verify the optimized models. Lastly, damage model based on Hashin Criteria is simulated in ABAQUS to correlate theoretical results with the experimental results.

Chapter 2: Methodology

This chapter elaborates the methodology of the research undertaken in this dissertation. The optimization of the machining process was executed in three broad steps. Firstly, it was the experimentation phase, followed by data analysis and optimization, thirdly simulation of the machining process was executed.

2.1 Process flow of research

Based on the literature review conducted to ascertain the research gaps and the objectives of the study, following research methodology was devised and is shown in Fig. 10. Firstly, experimentation is conducted based on Taguchi Design of Experiments Orthogonal array. Secondly, based on the experimental results optimization is carried out using ANOVA and GRA. And finally, a numerical model is developed to predict deformation and failure in honeycomb core structures.

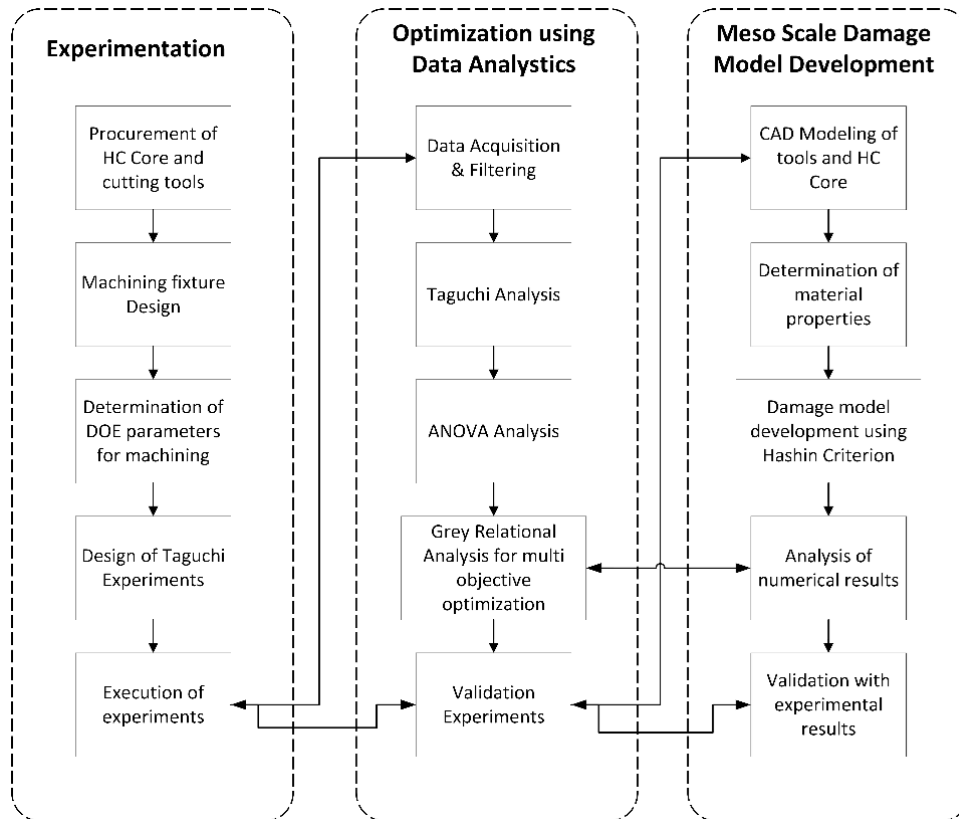


Figure 10 Methodology of Research

2.2 Experimentation

2.2.1 Tool, Workpiece, and machine

The workpiece material used in the study is the Nomex Honeycomb core which is produced by using aramid fibers. The selected honeycomb core has thin fibers and is manufactured by soaking the aramid fibers in phenolic resin (C. Li et al., 2022). The cores thus produced have continuous features of expanded aramid sheets which are glued together to form the hexagonal structure. This results in a lightweight and rigid structure that has high compression strength (Song et al., 2021)(Z. Li & Ma, 2020). The geometrical properties of the honeycomb core selected are given in Table 2. The Honeycomb core sheet is shown in Fig. 11.

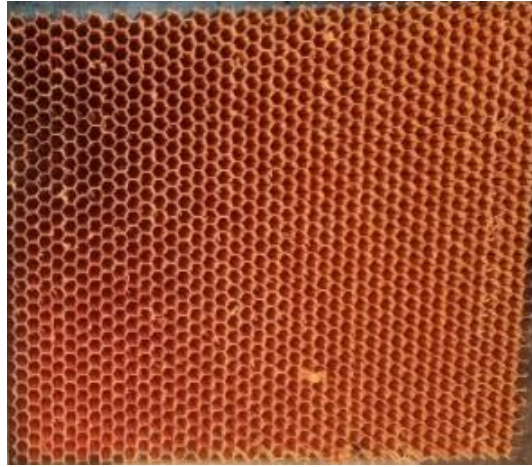


Figure 11 Nomex Honeycomb Core Block

Table 2 Geometrical Properties of Nomex Honeycomb Core

Designation	Density [Kg/m ³]	Cell Size [mm]	Wall thickness [μm]	Angle [°]
A10-48-5	48	5	80	120

There are many cutting tools available in the market to cut honeycomb cores depending on the type of material they are produced (HEXCEL, 2015), the machining operation that needs to be carried out, and the final finish required. For this research, the cutting tool chosen is manufactured by CoreHog®, America (*Medium Size Finishing Tools-CoreHoggers*, n.d.). The cutting tools are called medium-sized finishing tools and consist of two parts, one is the main shredder/hogger body made from solid Carbide, and the other is a medium core slicer or a disc cutter that is coated with TiCN. The tool is recommended to be used for milling operations. The tool specifications are

mentioned in Table 3. The geometry of the tool is shown in Fig. 12.

Table 3 Specifications of Cutting Tool

Sr. #	Part Name	Reference	Dia (D1)	Length of Cut (L2)	Shank Diameter (D2)	Overall Length (L1)	Core Slicer (D3)
1.	Medium CoreHogger	16MMHA-CARB	16mm	30mm	16mm	120mm	----
2.	Medium CoreSlicer (Smooth)	75CS	----	----	----	----	19mm



Figure 12 Cutting Tool Nomenclature

The machine utilized for the cutting operation was a 3-axis vertical CNC machine manufactured by YDPM. It has the bed size of 1180 x 560 mm and the controller is of Fanuc. The maximum spindle speed of the machine is 8000 rpm and can be enhanced using specialized spindles. Fig. 13 depicts the CNC machine utilized for the experiments.



Figure 13 CNC Machine of YDPM

2.2.2 Machining Fixture

For the measurement of force Bran Sensor Tri-axial force transducer based on a strain gauge sensor was used. Fixture plate was designed to fasten the honeycomb core during machining and this plate was then mounted on the transducer plate of the sensor. The design of the plate is depicted in Fig 4 (a-c).

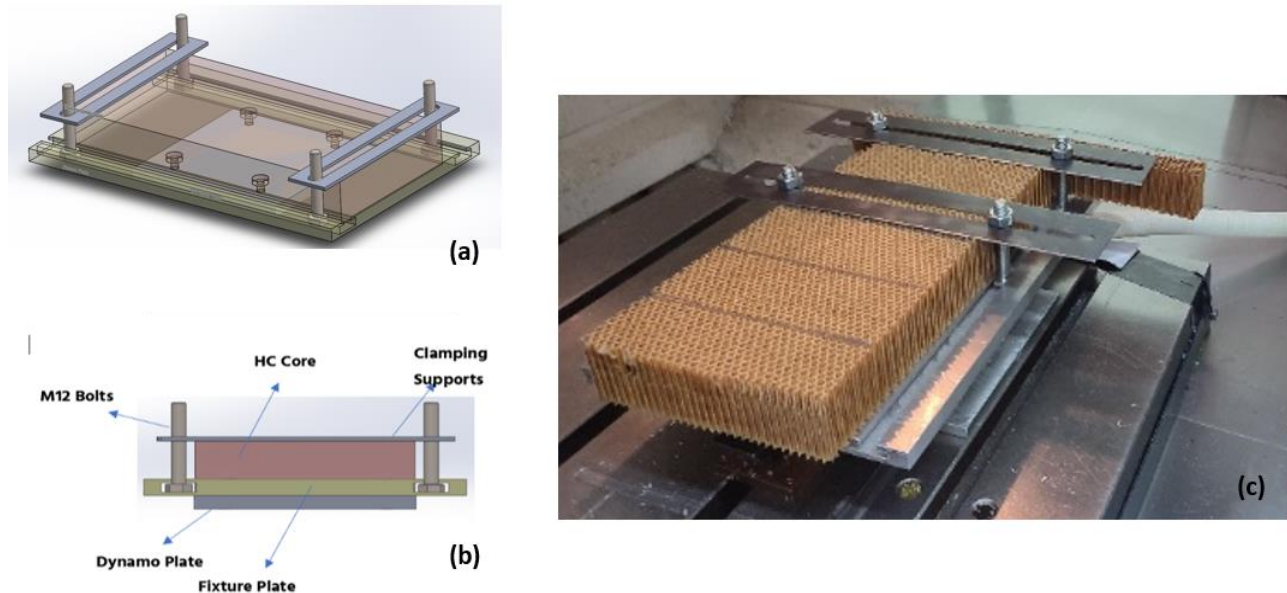


Figure 14 (a) Isometric view of Fixture Plate; (b) Front view of fixture plate; (c) Actual Experimental Setup

2.2.3 DoE parameters for machining

During the literature review, various research papers were studied and analyzed for the process parameters that greatly influenced the machining of honeycomb core structures (Shivakumar et al., 2020). It was revealed that most of the authors including Jaafar et. al and Tarik et al. (Zarrouk, Salhi, Atlati, et al., 2021) (Zarrouk et al., 2020) have used feed rate, and spindle speed to measure their effect on the machining forces. However, the literature review revealed that the Depth of Cut has not been considered in detail as an influencing factor of machining forces during experimental analysis. Therefore, this parameter along with other standard parameters (feed rate and spindle speed) were considered in this research to cover a wider array of influencing parameters.

Table 4 Taguchi Design of Experiments

Sr. #	Spindle Speed (SS) (rpm)	Feed Rate (FR) (mm/min)	Depth of Cut (DoC) (mm)
1.	5000	100	5
2.	5000	300	10
3.	5000	500	15
4.	6000	100	10
5.	6000	300	15
6.	6000	500	5
7.	7000	100	15
8.	7000	300	5
9.	7000	500	10

For the determination of levels against each parameter/factor, literature was studied (Z. Wang et al., 2017), and it was observed through trial and error, that greater spindle speed yields better cutting width and lesser forces. The comparison of different speeds against the forces in x-direction was made and is shown in Fig 15. Furthermore, utilizing statistical optimization to enhance processes is an important function of quality engineering. Taguchi wields an important cornerstone in this area because of its ability to design experiments with minimum iterations while yielding statistically significant results. This results in efficient resource-saving and timesaving. Owing to these characteristics Taguchi's Design of Experiments was utilized in the current research. Specifically, L9 orthogonal array was used to design the iterations of the experiments. The Taguchi L9 array along with the levels are depicted in Table 4-5.

Table 5 Parameters for DoE

Sr. #	Parameter	Level 1	Level 2	Level 3
1.	Spindle Speed (rpm)	5000	6000	7000
2.	Feed Rate (mm/min)	100	300	500
3.	Cutting Depth (mm)	5	10	15

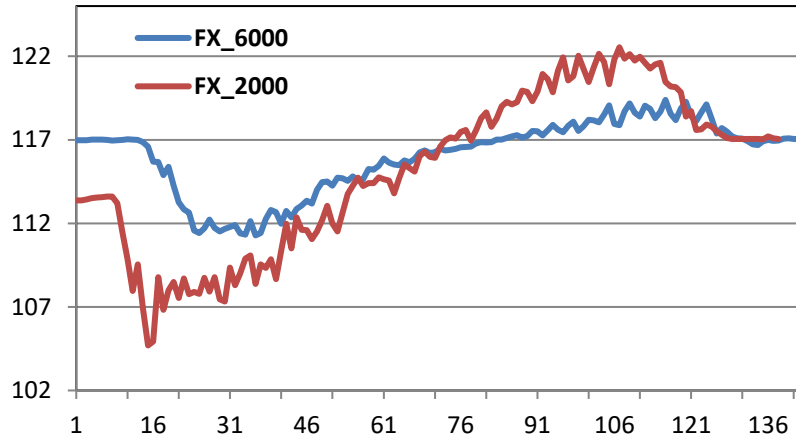


Figure 15 Trial Run Results for Forces in X-Axis

2.2.4 Response Variables and Measurements

The literature review suggests that the most important factor during machining is force (Jaafar et al.). Tearing, fraying, and delamination are some of the phenomena which occur during the machining of the honeycomb core. To ascertain their influence Cutting Efficiency (CE) was also considered as a response variable for this optimization study. The force was measured using Bran Sensor Tri-axial force transducer. The dynamometer was mounted on a fixture plate and was placed on the machine bed and force was measured on each axis. Before the actual measurements voltage factor was calculated for 1 N of force by applying a known load of 1 N in each direction. The voltages measured afterward were divided by this factor to obtain the force in newtons. For each experiment, the three force components were measured. The value in newtons was found by the difference between the minimum and maximum values (in millivolts) (1). Each configuration of the experiment was run two times and the average of each run was also taken. Afterwards the resultant force was calculated using (2).

$$Force(F_{x,y,z}) = Average_{2\ Exp} (\text{Max (mV)} - \text{Min (mV)}) \quad (1)$$

$$\text{Resultant Force } (F) = \sqrt{F_x^2 + F_y^2 + F_z^2} \quad (2)$$

For the measurement of cutting efficiency, the image dimension measurement system of Keyence (Fig. 16,17) was utilized and measurements of cutting widths were taken. Afterward, the measured cutting width was divided by the shredder diameter to obtain the cutting efficiency. The

equation (3) depicts the calculation formula. The cutting width was measured by fitting a line on the cut honeycomb for each experiment slot and measuring the width of the cut. Subsequently, the same is divided by the shredder diameter to find out the cutting efficiency. It is maximum when it approximates the shredder diameter and minimum when it deviates from the shredder diameter.

$$\text{Cutting Efficiency (CE)} = \frac{\text{Measured Cutting Width}}{\text{Shredder Dia}} \quad (3)$$



Figure 16 Keyence Image Dimensional Measurement System

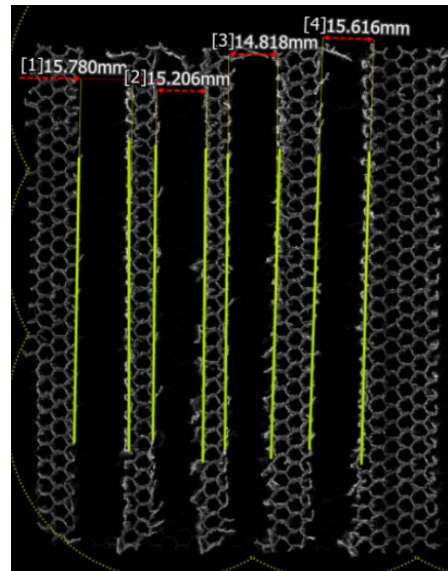


Figure 17 Measurements from Keyence system

2.3 Data Analytics and Optimization

The descriptive analysis was carried out using comparison of means, analysis of response tables from Taguchi Analysis. The steps of carrying out Taguchi analysis is elaborated in Fig.18. The response tables were analyzed to find out the individual significance of each parameter on Force and Cutting Efficiency. Afterwards, for the determination of variance in the data and to find out the percentage contribution ANOVA analysis was conducted. The steps for carrying out ANOVA analysis are elaborated in Fig. 19.

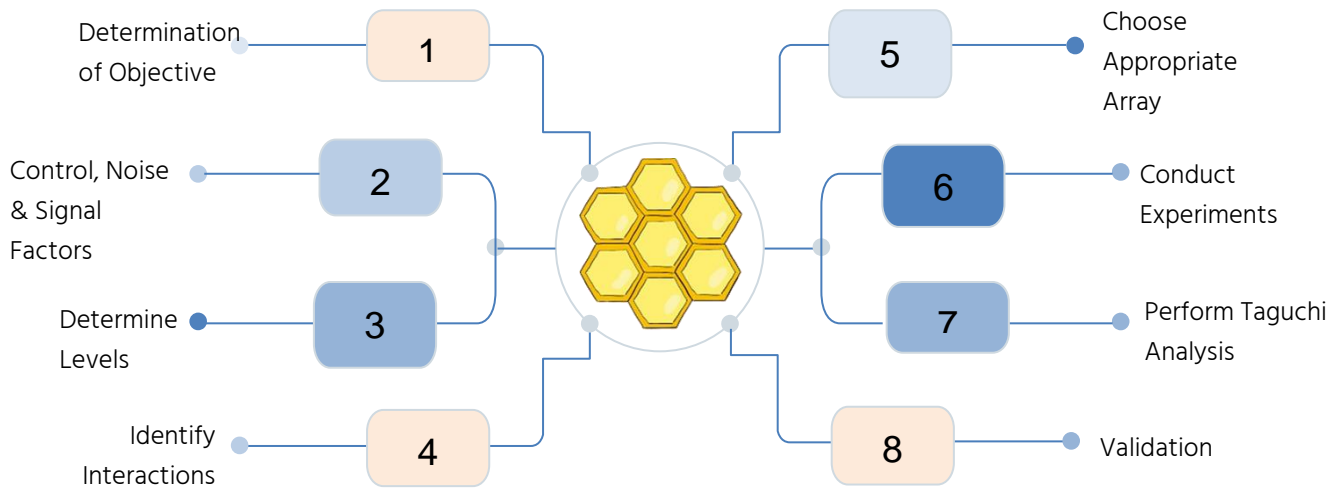


Figure 18 Steps for Taguchi Analysis

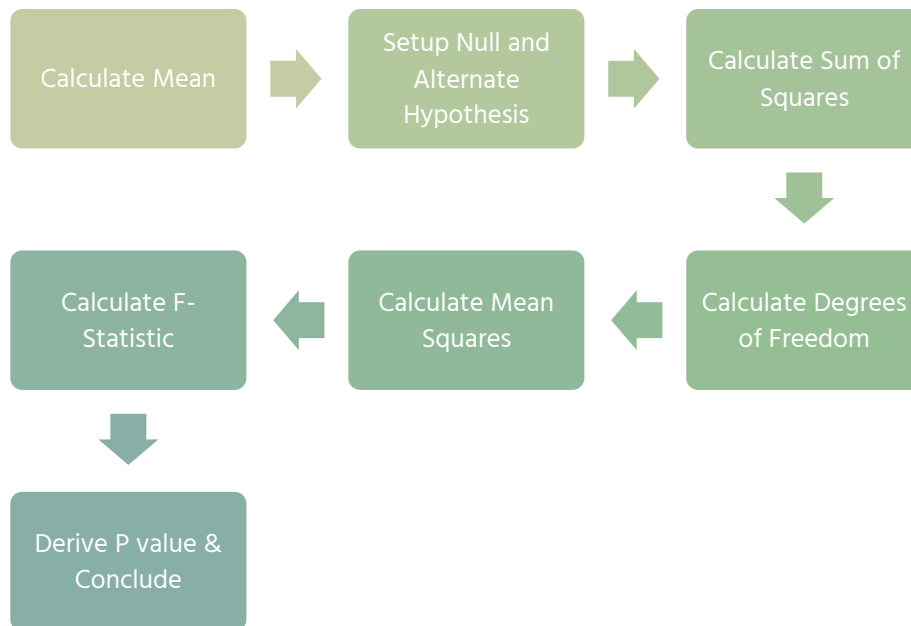


Figure 19 Steps for ANOVA Analysis

2.3.1 Desirability Function Analysis

Response Optimization tool of Minitab allows multi response optimization based on the

target values and weightage defined by the user. It works based on calculating the desirability function, this function can be used to optimize multiple responses which cannot be done using other methods of optimization (Vijayakumar & Pannirselvam, 2022).

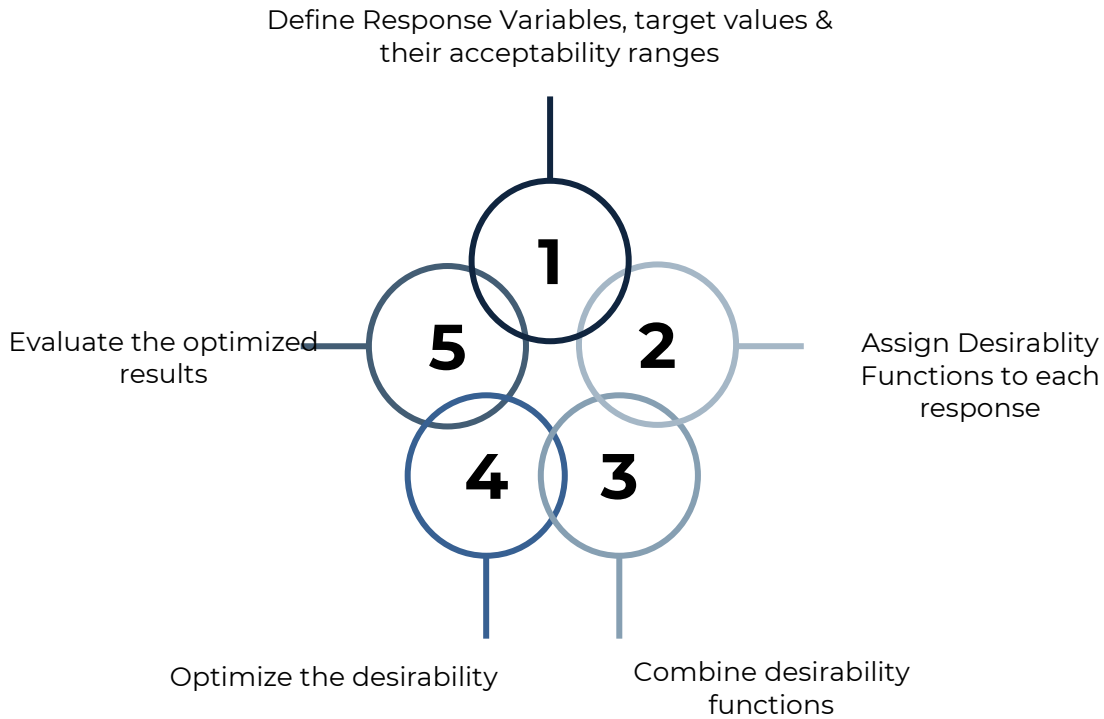


Figure 20 Steps for Desirability Function Analysis

This desirability value represents how well the combination of factor settings achieves the desired response for each variable. The desirability function considers both target values and acceptable ranges for each response variable. The steps of performing the desirability function analysis are shown in Fig. 20. First of all, in order to calculate the desirability function we need to define the response variables, their acceptable ranges and target values. Usually, this is calculated by using the maximum and minimum values of the response variables.

Then, desirability function for individual variables is calculated using smaller the better, larger the better or nominal the better criteria and finally the composite desirability is calculated using the geometric mean of the individual desirability functions.

2.3.2 Grey Relational Analysis

Grey Relational Analysis (GRA) is a useful tool that is extensively used in multi criteria decision making and multi objective optimization. It is a part of Grey System Theory which is an effective tool for prediction and forecasting in scenarios where there is little information available (Ju-Long, 1982). The GRG function was calculated based on the steps elaborated in Fig. 21.

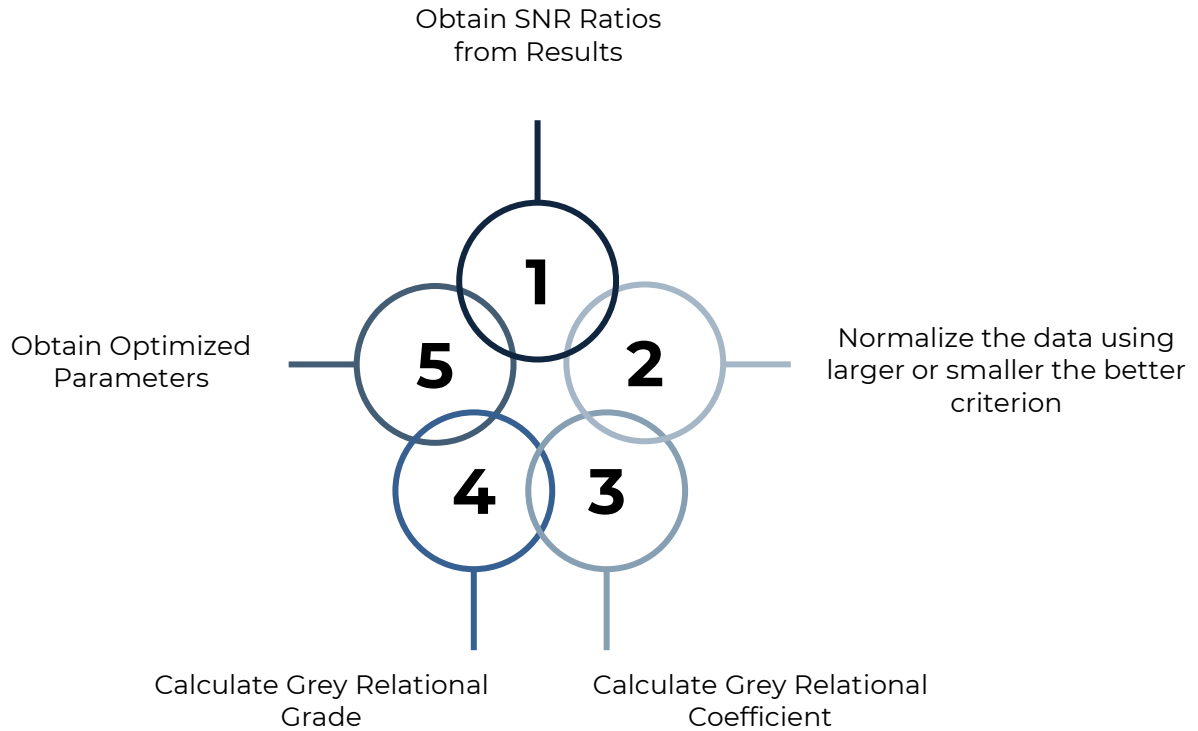


Figure 21 Steps for GRA

First, the data was normalized based on the equation 4-5. Normalization is done to compare the dataset points on a common scale (Modi & Bhavsar, 2023). For our purpose, we used max-min criteria to normalize the data which involves maximization of the datapoints or minimization of the datapoints. In case of force, we want to minimize the normalized data therefore equation 4 was used. In the case of cutting efficiency, maximization was needed and therefore, equation 5 was used to perform data normalization.

$$x_{ij} = \frac{\max(y_{ij}) - y_{ij}}{\max(y_{ij}) - \min(y_{ij})} \quad (4)$$

$$x_{ij} = \frac{y_{ij} - \min(y_{ij})}{\max(y_{ij}) - \min(y_{ij})} \quad (5)$$

Afterward, the deviation sequence was calculated based on the equation 6. The deviation sequence is the deviation of the normalized values of the datapoints from the ideal values or ideal series of values. For the force and cutting efficiency, the ideal value is 1. Therefore, the difference of each data point is calculated from 1. Later, the GRA coefficient was calculated, by using the equation 7. The GRA coefficient basically outlines the similarity between each input factor and the ideal values. After the calculation of the GRA Coefficient, the Grey Relational Grade (GRG) is calculated to find out the greyness of the data points. Equation 8 is used to find the GRG.

$$\Delta_{ij} = |1 - y_{ij}| \quad (6)$$

$$\zeta_{ij} = \frac{\Delta_{min} + \zeta \Delta_{max}}{\Delta_{ij} + \zeta \Delta_{max}} \quad (7)$$

$$\gamma_i = \frac{1}{n} \sum_{k=1}^n \zeta_i(k) \quad (8)$$

2.3.3 Prediction and validation of results

The predictions were calculated based on Minitab's prediction tool that is based on ANOVA scheme. After performing ANOVA and determining that there were significant differences among groups, one could proceed to fit a regression model to predict future outcomes or make inferences. Depending on the data and the nature of the problem, various regression models, such as linear regression, multiple regression, or nonlinear regression, could have been chosen.

In the regression model, the predictor variables (independent variables) that were believed to influence the dependent variable were specified. These predictor variables were typically the factors or variables that were part of the ANOVA analysis. Using statistical software like Minitab, the regression model was fitted to the data, and the software estimated the coefficients for each

predictor variable.

Once the model was fitted, it could be used to make predictions. For example, values for the predictor variables (based on new data or scenarios) could be input into the regression equation to predict the expected outcome (dependent variable). The accuracy of the regression model's predictions was assessed. Common metrics for this purpose included R-squared (to measure the goodness of fit), residuals analysis, and hypothesis tests for the significance of individual predictors. Finally, the predictions made by the regression model could be interpreted. These predictions could be used for various purposes, such as forecasting, decision-making, or understanding the relationships between variables. Based on the optimized results validation run was carried out to verify the predicted values.

2.4 Simulation and damage model development

The first step was to create a 3D model of the honeycomb core and the machining toolpath. This involved defining the core's geometry and specifying the tool's path. Material properties for both the honeycomb core and the machining tool were assigned to the simulation. These properties included the material's mechanical behavior, such as Young's Modulus, Poisson's Ratio, and thermal properties if heat generation was a factor. Appropriate boundary conditions were applied to the model. This included fixing certain faces or nodes to represent clamping or constraints on the core during machining.

The cutting forces, feed rates, and speeds for the machining tool were defined as loads. These inputs were based on the specific machining process being simulated. Contact interactions between the tool and the honeycomb core were established. This step was crucial for accurately representing the machining process, considering factors like friction and heat generation at the tool-core interface. The simulation parameters, including the time step, were configured. Appropriate analysis types, such as implicit or explicit dynamics, were chosen based on the nature of the machining process (e.g., static or dynamic). The model was then meshed, dividing it into finite elements to represent the physical structure.

The simulation was run to model the material removal process. The tool's interaction with the core was tracked over time to simulate the machining operation. In Abaqus, this might involve setting up a material removal subroutine or user-defined element deletion criteria to represent the

chip formation. During and after the simulation, relevant data, such as cutting forces, temperature distributions, and deformation, were recorded. Post-processing tools in Abaqus were used to visualize and analyze the results. Once the simulation accurately represented the machining process, a final analysis was performed, and the results were documented in a report. This report included details of the simulation setup, methodology, and key findings.

Chapter 3: Results and Discussion

This chapter outlines the results of the experiments conducted during this research based on the methodologies discussed in the previous chapter. Afterwards, the results of multi-objective optimization are enumerated and discussed in detail.

3.1 Experimental results

The experiments were conducted as per the runs mentioned in Table 4, and the response variables were measured using the force transducer and Keyence machine. The compiled results are elaborated in Table 6. The resultant force was calculated according to Eq. 2 and CE was calculated as per Eq. 3.

Table 6 Experimental Results

Sr. #	Spindle Speed (rpm)	Feed Rate (mm/min)	Depth of Cut (mm)	F _x	F _y	F _z	F	CE
1.	5000	100	5	11.82	4.66	11.61	17.22	0.87
2.	5000	300	10	16.69	5.88	14.78	23.06	0.97
3.	5000	500	15	21.51	7.44	16.60	28.17	0.99
4.	6000	100	10	7.52	5.27	6.31	11.14	0.96
5.	6000	300	15	13.22	8.94	14.03	21.24	1.01
6.	6000	500	5	17.30	6.71	16.98	25.15	0.87
7.	7000	100	15	6.93	4.77	7.07	10.99	0.97
8.	7000	300	5	11.63	5.44	10.65	16.68	0.89
9.	7000	500	10	13.62	7.21	13.30	20.35	0.91

3.2 Data Analytics

The comparison of means graph is depicted in Fig 22-23. The graph at Fig. 22 indicates the comparison of means of FR and SS. The trend is visible positive relation of feed rate vis-à-vis the resultant force. Whereas there is a negative relation between SS and resultant forces. Similarly, Fig. 23 indicates a linear positive trend of the DoC vis-a-vis the CE, whereas the SS and FR are not positively correlated.

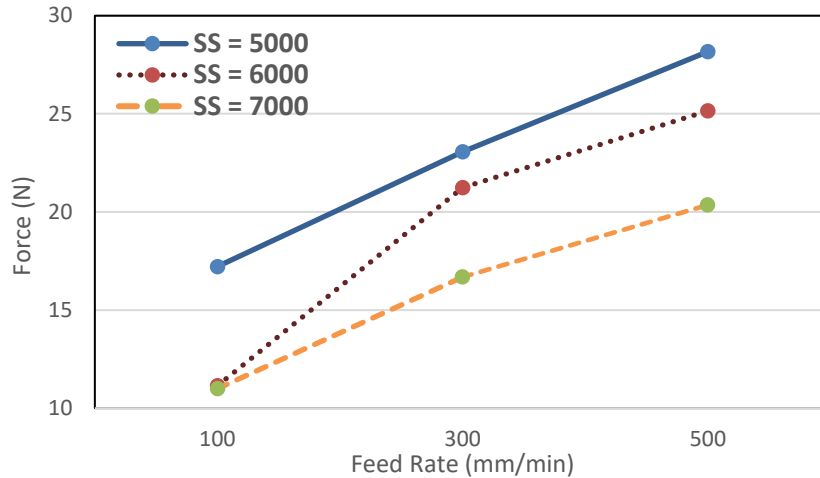


Figure 22 Feed Rate vs Force (F) vs Spindle Speed

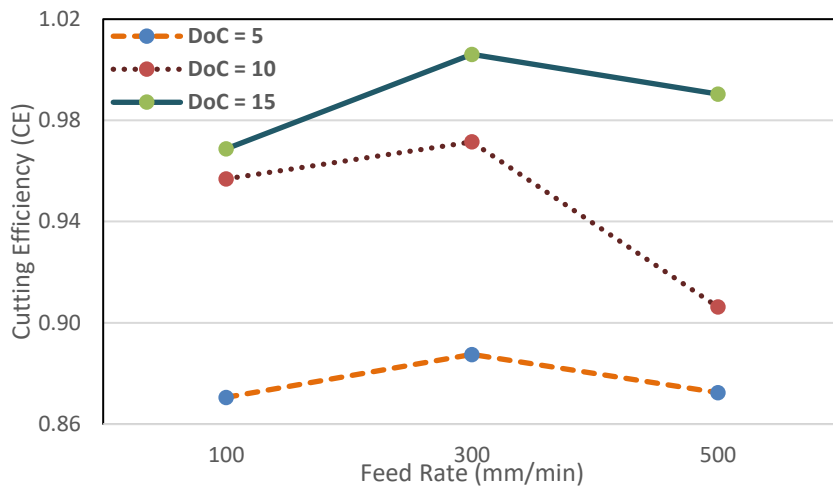


Figure 23 Feed Rate vs Cutting Efficiency vs Depth of Cut

Afterwards, Taguchi Analysis of the variables was carried out and the results are tabulated in Table 7-8. The response tables from Taguchi Analysis indicate that the most significant factor effecting the forces on the tool is FR followed by SS and DoC, whereas, in case of CE, DoC is the most significant factor followed by FR and SS. The ANOVA Analysis of the factors was carried out and the results are tabulated in Table 9-10. The results reveal that for forces the p-value is most significant for FR (0.01) followed by SS (0.029) and DoC (0.247). Whereas, in the case of Cutting Efficiency, the p-value is most significant in the case of DoC (0.023) followed by FR (0.217) and SS (0.285). The main effects plot of S/N ratios are depicted in Fig. 24(a-b). The plots endorse the results of the response tables and significant values indicating similar trends vis-à-vis cutting

forces and cutting efficiency. Based on the ANOVA tables the percentage contribution of each factor was also calculated and it is depicted in the Table 11.

Table 7 Response Table for SN Ratios (Force)

Level	SS (rpm)	FR (mm/min)	DoC (mm)
1	-26.99	-22.16	-25.72
2	-25.17	-26.08	-24.79
3	-23.81	-27.73	-25.45
Delta	3.18	5.57	0.94
Rank	2	1	3

Table 8 Response Table for SN Ratios (CE)

Level	SS (rpm)	FR (mm/min)	DoC (mm)
1	-0.513	-0.6209	-1.1421
2	-0.5051	-0.4117	-0.4964
3	-0.7225	-0.7079	-0.1021
Delta	0.2174	0.2963	1.0399
Rank	3	2	1

Table 9 ANOVA Table of S/N ratios for F

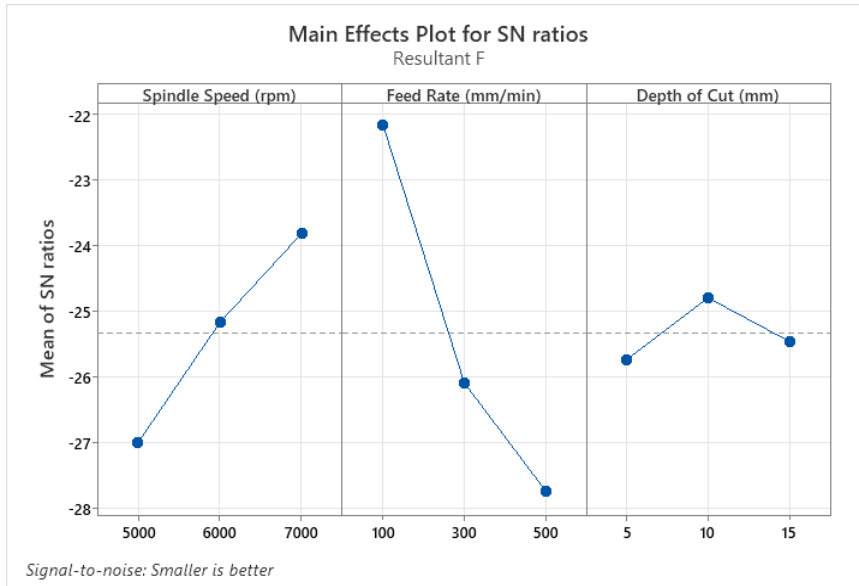
Source	DF	Adj SS	Adj MS	F-Value	P-Value
SS (rpm)	2	69.566	34.783	33.98	0.029
FR (mm/min)	2	200.798	100.399	98.09	0.01
DoC (mm)	2	6.25	3.125	3.05	0.247
Error	2	2.047	1.024		
Total	8	278.661			

Table 10 ANOVA Table for S/N ratios for CE

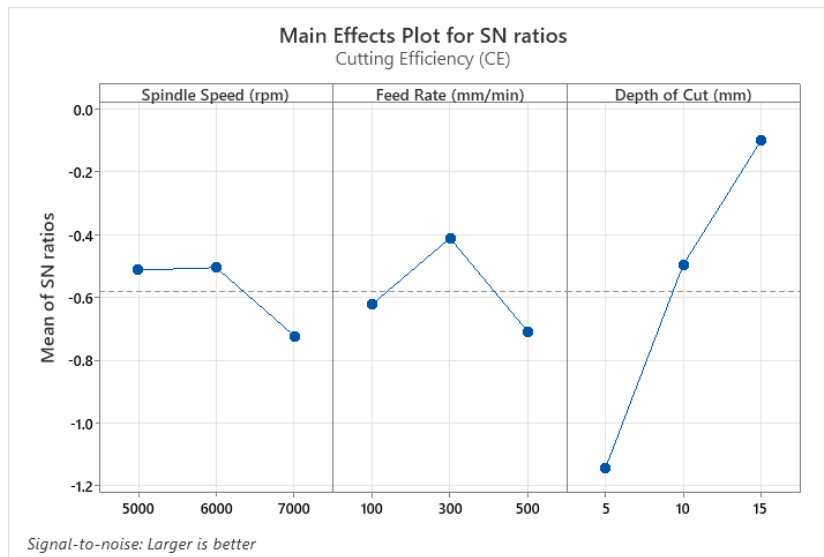
Source	DF	Adj SS	Adj MS	F-Value	P-Value
SS (rpm)	2	0.001136	0.000568	2.51	0.285
FR (mm/min)	2	0.001632	0.000816	3.61	0.217
DoC (mm)	2	0.018983	0.009492	41.94	0.023
Error	2	0.000453	0.000226		
Total	8	0.022204			

Table 11 Percentage Contribution based on ANOVA

Factors	% Contribution F	% Contribution CE
Spindle Speed (rpm)	24.96	5.12
Feed Rate (mm/min)	72.06	7.35
Cutting Depth (mm)	2.243	85.49



(a) Force



(b) CE

Figure 24 Main Effects Plot for S/N ratios (a) Force & (b) CE

Cutting Nomex® Honeycomb core results in various defects as highlighted in the studies of Liu et al. (Liu et al., 2015). These defects are responsible for higher cutting forces in case the feed rate is increased. The Nomex HC core is made up of aramid fibers and these fibers have high hardness values. When feed rate is increased, the contact area of tool with the fibers increases resulting in increased shearing forces. Jaafar et al. (Jaafar, Makich, et al., 2021) and Tarik (Zarrouk,

Salhi, Nouari, et al., 2021) have concluded similar results through simulation of the machining process and have shown that at higher feed rates the cutting force increase while the chip size tends to be smaller (Zenia et al., 2015) (Roy, Nguyen, et al., 2014). Similarly, in the case when DoC is increased the accumulation of material results in increased shearing forces. The accumulation of the material is due to the elastoplastic behavior of the HC core. However, this accumulation is reduced when spindle speeds are high, tending to reduce the cutting forces (Xu et al., 2021).

ANOVA shows that DoC is the most important factor in the case of CE. It is because the DoC allows uniform material removal from top and bottom of the cut. The uniformity of the cut is because greater length of the shredder is engaged during cutting resulting in better CE. The results in Table 10 clearly indicate this correlation as DoC is the prime significant factor when it comes to the calculation of CE. Similar results were reported through simulations by Tarik et al. (Zarrouk, Salhi, et al., 2022).

3.3 Multi-Objective Optimization

The optimization of machining parameters is essential for several reasons. Firstly, Nomex honeycomb core exhibits unique mechanical properties that are influenced by machining parameters undertaken by the current research (Roy, Park, et al., 2014). The appropriate selection of these parameters can significantly impact the structural behavior of the core material when sandwiched structures are to be produced through it (Zinno et al., 2011). Secondly, optimization techniques allow for the identification of the optimal combination of machining parameters that minimize forces, enhances material properties and cutting efficiency, and improves overall structural integrity (Girolamo et al., 2018).

3.3.1 Desirability Function Analysis (DFA)

For the purpose, Desirability Function Analysis (DFA) was used to optimize the response variables in relation to the influencing factors. The goal of this technique is to calculate the desirability function that optimizes multiple response. This desirability value represents how well the combination of factor settings achieves the desired response for each variable. The desirability function considers both target values and acceptable ranges for each response variable (Vijayakumar & Pannirselvam, 2022). Based on the steps elaborated in 2.3.1 the desirability

function was calculated and response was optimized using Minitab® Response Optimizer. The optimized results with composite desirability of 86% are tabulated below in Table 12.

Table 12 Response Optimization through Composite Desirability Function

Solution	Spindle Speed (rpm)	Feed Rate (mm/min)	Depth of Cut (mm)	CE Fit	F Fit	Composite Desirability
1	6000	100	15	0.992211	13.7624	0.86761

3.3.2 Grey Relational Analysis

Similar to DFA, Grey Relational Analysis (GRA) is a useful tool that is extensively used in multi criteria decision making and multi objective optimization. It is a part of Grey System Theory which is an effective tool for prediction and forecasting in scenarios where there is little information available (Ju-Long, 1982). The GRG function was calculated based on the steps elaborated in the 2.3.2. The calculations based on the steps highlighted are compiled in Fig. 25.

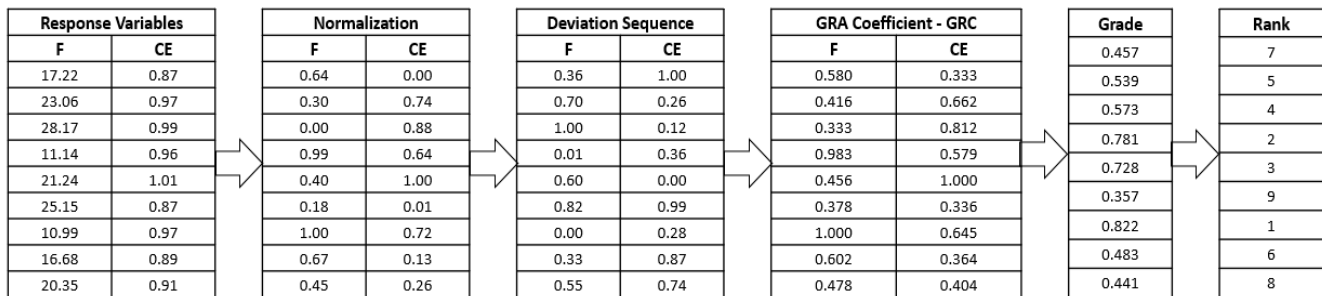


Figure 25 Results of Grey Relational Analysis

After calculating the GRG, the ranking was performed based on the maximum GRG value. The ranking is also shown in Fig 25. Finally, response tables were calculated based on GRG value to find the optimum parameters from the GRG function. The Table 13 outlines the response table and Table 14 outlines the optimum parameters. The optimum levels from both the techniques come out to be 6000 rpm for SS, 300 mm/min for FR and 15 mm for DoC.

Table 13 Response Table for GRG

Parameters	1	2	3
Spindle Speed (rpm)	0.5227473	0.621995504	0.582108
Feed Rate (mm/min)	0.6866603	0.583130409	0.457061
Cutting Depth (mm)	0.4320547	0.587107776	0.707689

Table 14 Optimum Levels based on GRG & DFA

Optimum Levels	DFA Based	GRG Based
Spindle Speed (rpm)	Level 2	Level 2
Feed Rate (mm/min)	Level 1	Level 1
Cutting Depth (mm)	Level 3	Level 3

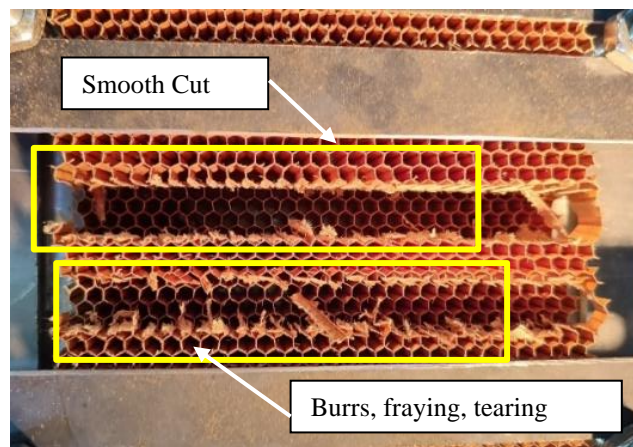


Figure 26 Top cut represents run 7 (best run) bottom cut represents run 6 (worst run)

The visual results of the worst and best experimental runs are shown in Fig 26 for best and worst runs whereas the visual results are combined for each experiment Appendix A. It can be observed from the results that the best results (Experiment # 7) are without burrs, protrusions, the cut fiber is smooth, and the cut width is accurately achieved. For the worst experimental run (Experiment # 6) it can be seen there is fraying, burrs and uncut fibers visible whereas, the cutting efficiency is badly affected. The results strongly correlate with quantitative analysis. As indicated earlier as the feed rate increases the time of contact between cutter and workpiece decreases,

restricting the smooth execution of the cut. Whereas the opposite is true in case of run 7 as the feed rate decreases it allows maximum material removal time, decreasing burrs and fraying.

After optimum parameters were calculated based on the optimization techniques, the results of forces and cutting efficiency were predicted and the predicted results are tabulated below in Table 15. The prediction was calculated using Minitab’s prediction function for ANOVA. For predictions using ANOVA in Minitab, the software calculates the means or fitted values for different factor levels or combinations based on the estimated coefficients and the observed data. These predictions represent the expected or average response for the specific factor settings. The predicted value for force was 13.76 N and the cutting efficiency was 0.99. The Standard Error Fit for force is 0.89 and cutting efficiency is 0.01 which is very low value indicating that the predicted values from regression model is a good fit.

Table 15 Predicted results from ANOVA

Prediction of Force and Cutting Efficiency (213)				
Parameter	Fit	SE Fit	95% CI	95% PI
F	13.7624	0.892221	(9.92347, 17.6013)	(7.95849, 19.5663)
CE	0.992211	0.013268	(0.935125, 1.04930)	(0.905905, 1.07852)

After determining the optimal process parameter settings, the final step involves predicting and verifying the enhancements in performance characteristics using these optimal settings. A validation experiment is carried out using the identified best parameter values to assess the combined objective. The results of the validation experiment run is depicted in Table 16. The results are within 5% error from the predicted results and shows the accuracy of the optimized parameters through both the optimization techniques. Furthermore, there is an improvement in the machining process by 47.8% for forces and 11.5% in case of cutting efficiency. The comparison of worst predicted and validated results are depicted in Fig 27.

Table 16 Validation Results

Response	Optimum Experiment Levels	Predicted Value	Validation Run	Worst Experimental Run	Percentage Error (Validated vs. Predicted)	Percentage Improvement (Worst vs. Predicted)
Force	213	13.76	13.11	25.15	4.70%	47.8%
CE		0.99	0.97	0.87	2.20%	11.5%

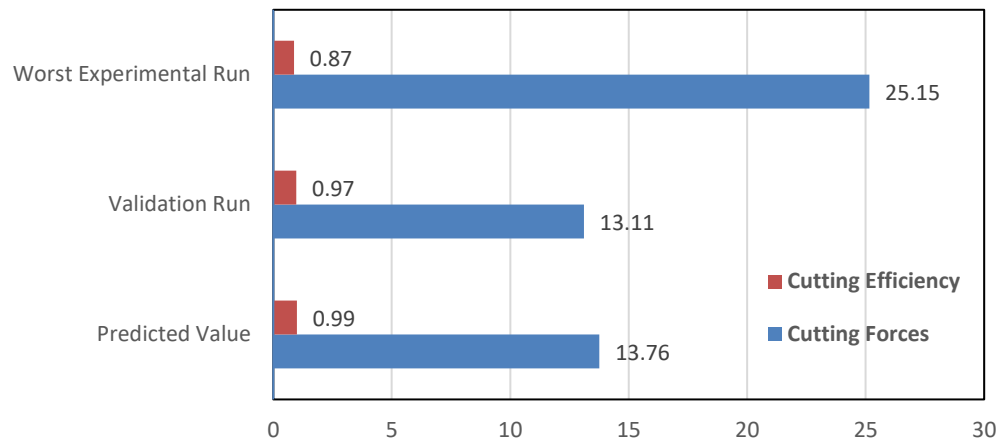


Figure 27 Comparison of predicted, validated and worst runs

3.4 Conclusion

In conclusion, this study focused on optimizing the milling operation for machining Nomex® Honeycomb core used in aerospace composite components. Through Taguchi-based Design of Experiments (DOE), ANOVA analysis, and correlation analysis, the influence of spindle speed, feed rate, and depth of cut on cutting forces and cutting efficiency was investigated. The results indicated that:

- ANOVA analysis indicates that the feed rate was the most significant factor with percentage contribution of 72% affecting cutting forces, whereas, depth of cut was most significant in case of cutting efficiency with percentage contribution of 85%.
- The significance of feed rate for cutting forces had a p-value of 0.01, followed by Spindle Speed 0.029 and Depth of Cut 0.247
- The depth of cut had a notable impact on cutting efficiency with a p-value of 0.023 followed by Feed Rate 0.217 and Spindle Speed 0.285.
- Composite Desirability was determined to be 86% indicating significance of optimization methodology.
- The results of Grey Relational Analysis (GRA) correlated with the DFA results and both techniques demonstrate similar optimal settings of response parameters. The

optimal settings were found to be 6000 rpm of spindle speed, 100 mm/min feed rate and 15mm Depth of Cut.

- ANOVA based prediction of parameters was found to be correct in comparison to the experimental validation results for the optimal settings and the error was within 5%.
- The percentage improvement in cutting forces was found out to be 47.8% as compared to the worst experimental run and cutting efficiency was improved by 11%.

This experimental study provides valuable insights into improving the accuracy and precision of cut profiles in Honeycomb Core (HC Core) machining, ultimately contributing to the enhancement of aerospace composite component manufacturing processes. There are, however, many vistas still unexplored in this area including the results of simulated / experimental studies on other machining / milling parameters of honeycomb core with different cutting tool geometries and different cut profiles.

Chapter 4: Simulation of Machining Honeycomb cores

This chapter outlines the simulation process for the machining of honeycomb core and elaborates its results. It highlights the properties used for the model, the damage criteria utilized to predict failure, boundary conditions, loading conditions and meshing to simulate the machining process.

4.1 Process of simulation

The simulation of machining process requires an understanding of the process in detail as this understanding is the cornerstone from which an effective simulation model can be built. The overview of this process is elaborated below:

The simulation process for machining a Nomex honeycomb core involves a series of carefully orchestrated steps to replicate the real-world machining operation. In this elaborate explanation, we will delve into the details, highlighting key aspects of the simulation process:

- Geometry and Toolpath Definition:

To commence the simulation, a 3D model of the Nomex honeycomb core and the machining toolpath was meticulously crafted. This model served as the digital representation of the core's intricate structure. The toolpath was specified to mirror the exact trajectory the machining tool would follow during the operation.

- Material Property Assignment:

Material properties played a pivotal role in ensuring the authenticity of the simulation. Young's Modulus, Poisson's Ratio, and thermal properties were attributed to both the Nomex honeycomb core and the machining tool. This step was crucial for emulating the mechanical behaviour of the materials accurately.

- Boundary Conditions:

To replicate the real-world machining setup, precise boundary conditions were imposed on the model. Specific faces or nodes were fixed to simulate clamping or constraints applied to the honeycomb core during machining.

- Load Definitions:

The cutting forces, feed rates, and machining speeds were defined as loads in the simulation. These load inputs were derived from the particulars of the machining process being replicated, capturing the dynamic nature of the machining operation.

- Contact Interactions:

One of the critical elements in the simulation was the establishment of contact interactions between the machining tool and the Nomex honeycomb core. These interactions factored in considerations like friction and heat generation at the tool-core interface, lending authenticity to the simulation.

- Simulation Parameters and Meshing:

The success of the simulation hinged on configuring simulation parameters like the time step and selecting the appropriate analysis type, whether implicit or explicit dynamics. Meshing the model into finite elements, meticulously dividing the structure, ensured that the physical reality was closely mirrored.

- Material Removal Simulation:

At the heart of the simulation lay the material removal process. The tool's interaction with the Nomex honeycomb core was tracked over time, mirroring the actual machining operation. This phase might have involved sophisticated techniques like material removal subroutines or user-defined element deletion criteria to simulate chip formation.

- Data Recording and Post-processing:

Data collection was continuous throughout and after the simulation. Crucial parameters such as cutting forces, temperature distributions, and deformation were recorded. Post-processing tools in the simulation software, such as Abaqus, were utilized to visualize and analyse these results, providing valuable insights into the behaviour of the honeycomb core during machining.

- Final Analysis and Reporting:

Following the successful simulation, a comprehensive final analysis was conducted. The results were meticulously documented in a detailed report. This report served as a comprehensive record of the simulation process, outlining the setup, methodology, and key findings.

4.2 Simulation of simple machining process

Firstly, the simulation of simple machining process was built using ABAQUS and it was seen what critical parameters are needed to build the simulation. For this simulation the tool used was

modelled in Solidworks and is shown in Fig. 28. After modelling the tool the same was imported in ABAQUS and simulation was run to cut an aluminium block. The simulation run was successful and is shown in Fig. 29. The damage model used for this simulation was Johnson Cook and the properties of the workpiece based on this damage model are shown in Table 17-18.

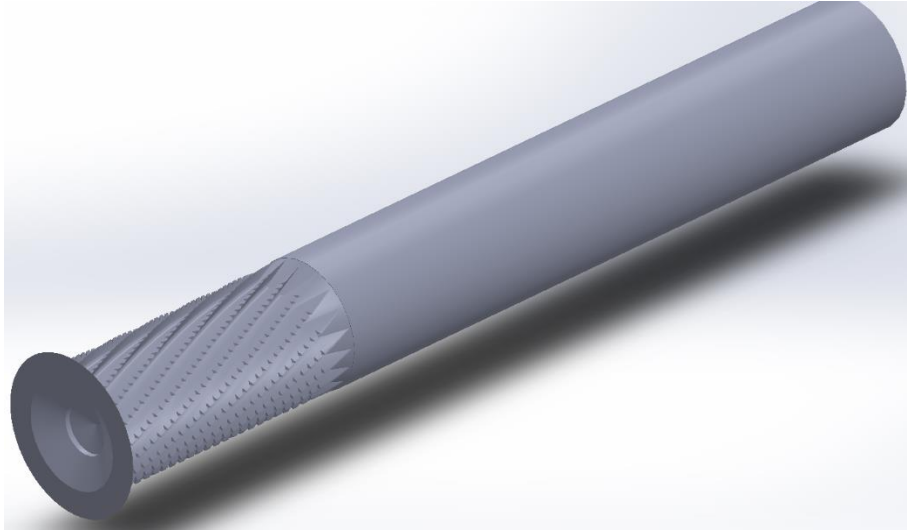


Figure 28 CAD Model of cutting tool

Table 17 Johnson Cook Material Properties for plasticity

A	B	n	m	Melting Temp	Transition Temp
324100000	113800000	0.42	0	0	0

Table 18 Constants for damage model based on the Johnson Cook Criteria

d1	d2	d3	d4	d5	Melting Temp	Transition Temp	Reference Strain
-0.77	1.45	-0.47	0	0	0	0	1

4.3 Evaluation of Hashin Damage Criteria

After the successful modelling of this process, based on the literature review presented in 1.7 and elaborated in 2.4 it was necessary to evaluate the damage model available to simulate specifically the failure of Nomex Honeycomb core structures. For this the most used damage model is Hashin Damage Criteria which is available in ABAQUS library for direct

implementation. The same was used to simulate the failure of a 2D composite sample built in ABAQUS. The results of the same are shown in Fig. 30-31

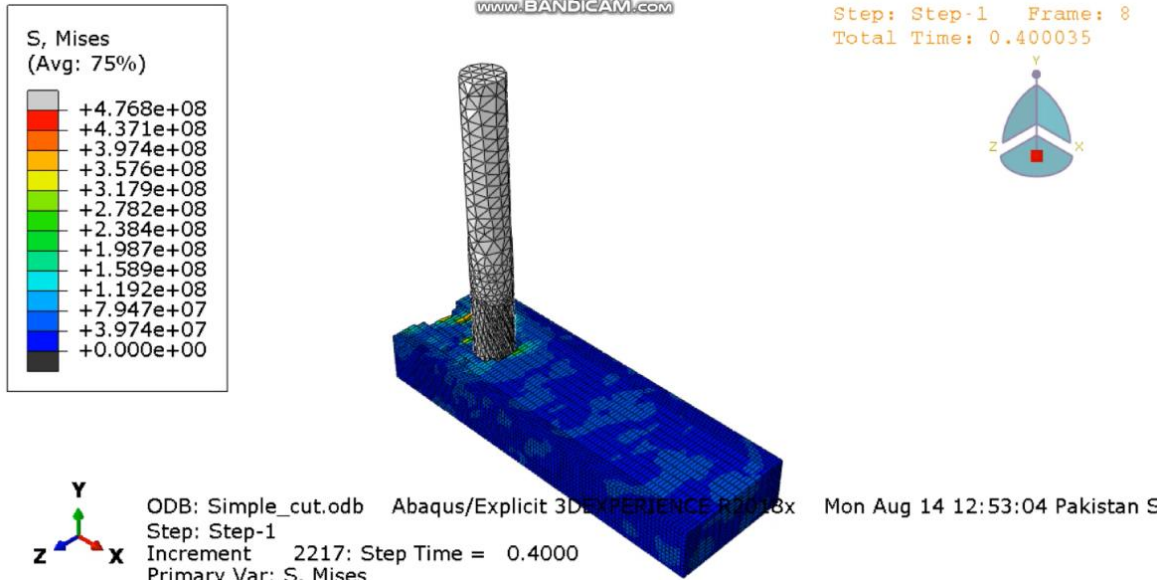


Figure 29 Simulation of Machining Process

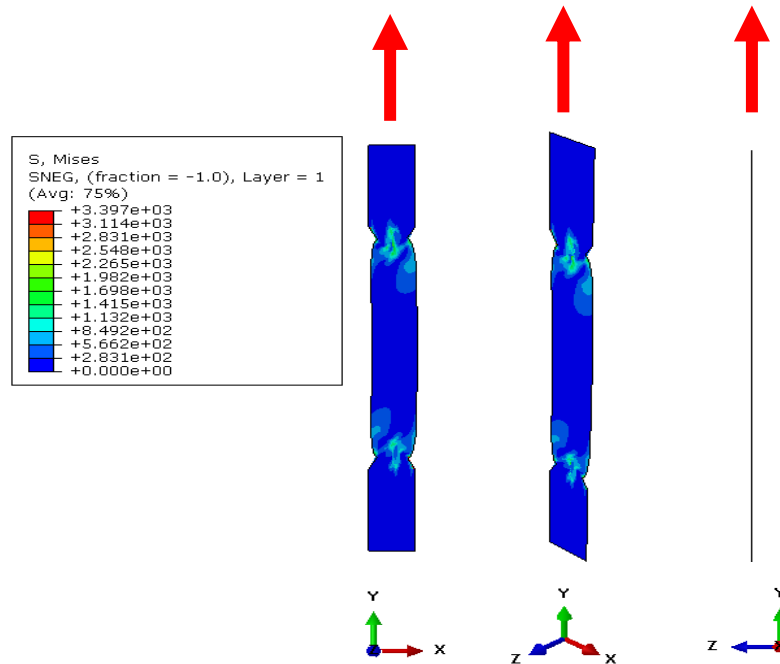


Figure 30 Simulation of 2D shell composite element using Hashin Damage Criteria

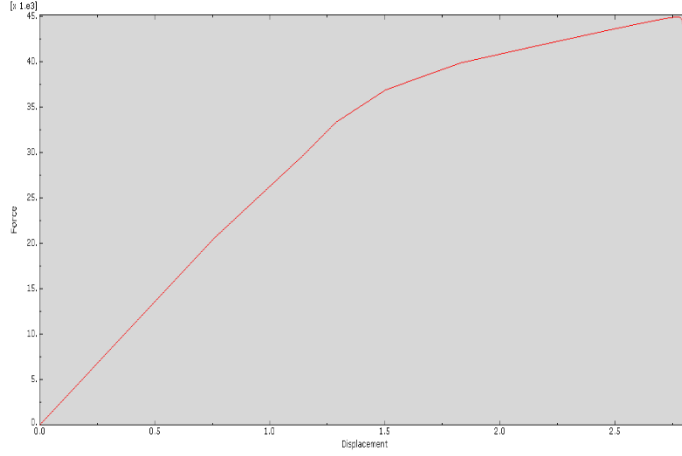


Figure 31 Results of Simulation

During simulation of the results it was revealed that there are two types of Hashin Damage Criterion available to predict the failure in composite laminate structures. 1) 2D Hashin Damage Criteria and 2) 3D Hashin Damage Criteria. The inbuilt criteria available in ABAQUS is 2D and is suitable to predict in-plane damage/failure and it does not take into account the out of plane stresses. The same can be deduced from the ABAQUS documentation available in its library through the following stiffness matrices.

Stress in σ_{xx} , σ_{yy} and τ_{xy} , d are their damage parameter. (inplane stress scenario)

$$d_f = \text{fiber}, d_m = \text{matrices}, d_s = \text{shear}$$

$$E_1 = \text{fiber}, E_2 = \text{matrices}, G_{12} = \text{shear}$$

$$\varepsilon_i = S_{ij} \cdot \sigma_j$$

$$\begin{Bmatrix} \varepsilon_1 \\ \varepsilon_2 \\ \gamma_{12} \end{Bmatrix} = \begin{bmatrix} \frac{1}{E_1} & -\frac{\nu_{21}}{E_2} & 0 \\ -\frac{\nu_{12}}{E_1} & \frac{1}{E_2} & 0 \\ 0 & 0 & \frac{1}{G_{12}} \end{bmatrix} \begin{Bmatrix} \sigma_1 \\ \sigma_2 \\ \tau_{12} \end{Bmatrix} \quad \mathbf{M} = \begin{bmatrix} \frac{1}{(1-d_f)} & 0 & 0 \\ 0 & \frac{1}{(1-d_m)} & 0 \\ 0 & 0 & \frac{1}{(1-d_s)} \end{bmatrix}.$$

However, for the explicit, dynamic modelling of Nomex Honeycomb core the 3D Hashin Criteria is needed to model the failure. The literature review (Jaafar, Nouari, et al., 2021) suggests that to implement this criteria 3D stresses are to be considered and the stiffness matrices for the same are shown below. These matrices depict failure in three dimensions and is suitable for

orthotropic properties of composite laminate structure which is the basis of construction of Nomex Honeycomb Core. To built a failure model of this sort subroutines needs to be written in VUMAT/UMAT to model the 3D Hashin Criteria. The orthotropic behaviour during machining is shown in Fig. 32. This requires extensive knowledge of coding and simulation which was not possible within the time frame of current dissertation.

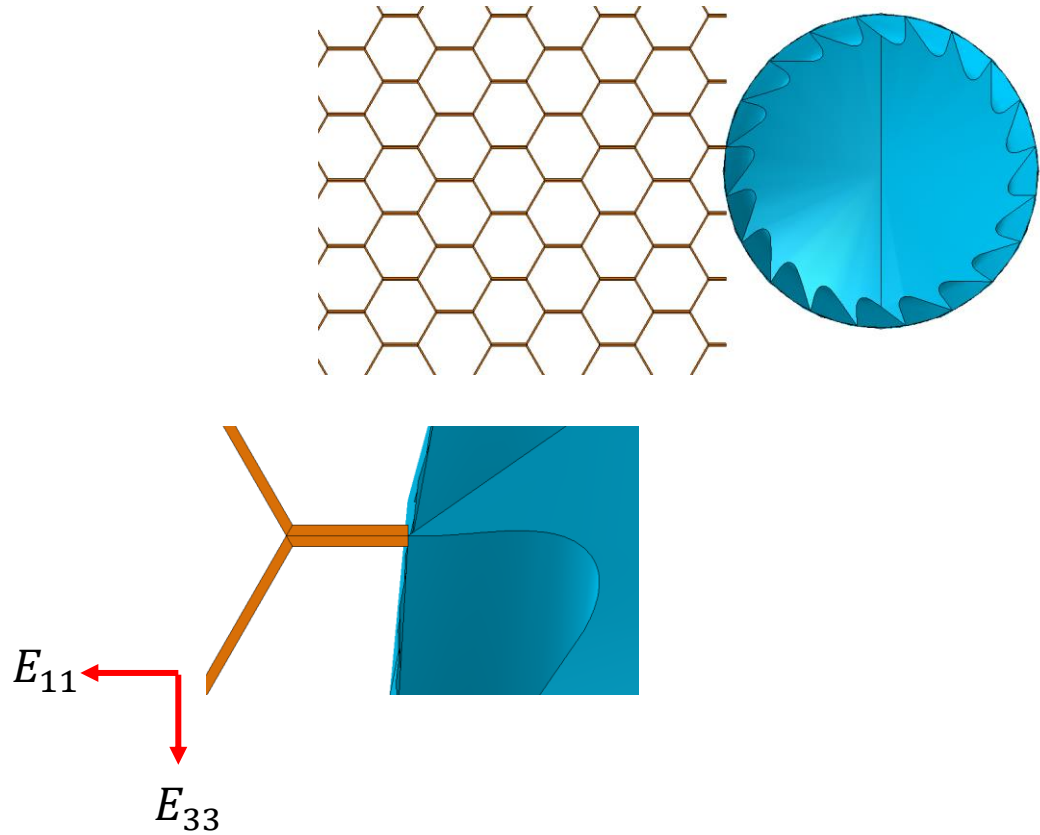


Figure 32 3D stresses during machining

$$S_{D,t_0} = \begin{bmatrix} \frac{1}{(1-D_{F,t_0})E_{11}} & -\frac{\nu_{12}}{E_{11}} & -\frac{\nu_{12}}{E_{11}} & 0 & 0 & 0 \\ -\frac{\nu_{12}}{E_{11}} & \frac{1}{(1-D_{M,t_0})E_{22}} & -\frac{\nu_{23}}{E_{22}} & 0 & 0 & 0 \\ -\frac{\nu_{12}}{E_{11}} & -\frac{\nu_{23}}{E_{22}} & \frac{1}{(1-D_{M,t_0})E_{22}} & 0 & 0 & 0 \\ 0 & 0 & 0 & \frac{1}{(1-D_{S,t_0})E_{12}} & 0 & 0 \\ 0 & 0 & 0 & 0 & \frac{1}{(1-D_{S,t_0})E_{12}} & 0 \\ 0 & 0 & 0 & 0 & 0 & \frac{2(\nu_{23}+1)}{(1-D_{M,t_0})E_{22}} \end{bmatrix}$$

$$M = \begin{bmatrix} \frac{1}{1-D_{F,t_0}} & 0 & 0 & 0 & 0 & 0 \\ 0 & \frac{1}{1-D_{M,t_0}} & 0 & 0 & 0 & 0 \\ 0 & 0 & \frac{1}{1-D_{M,t_0}} & 0 & 0 & 0 \\ 0 & 0 & 0 & \frac{1}{1-D_{S,t_0}} & 0 & 0 \\ 0 & 0 & 0 & 0 & \frac{1}{1-D_{S,t_0}} & 0 \\ 0 & 0 & 0 & 0 & 0 & \frac{1}{1-D_{M,t_0}} \end{bmatrix}$$

4.4 Simulation of Nomex Honeycomb Core

Based on the discussion above it was concluded that composite modelling cannot be carried out for simulation however, the honeycomb can be converted into a solid model and the properties of the Honeycomb determined by (Khan et al., 2021) can be used to build an equivalent representative model of honeycomb structure. However, that requires calibration of the available models in ABAQUS and this requires extensive time as well. Finally, the simulation was built using the available resources based on the Johnson Cook model considering the honeycomb structure as solid. The encastre constraint was applied to fix the honeycomb from all sides and a rigid body constraint was applied to tool Fig. 33.

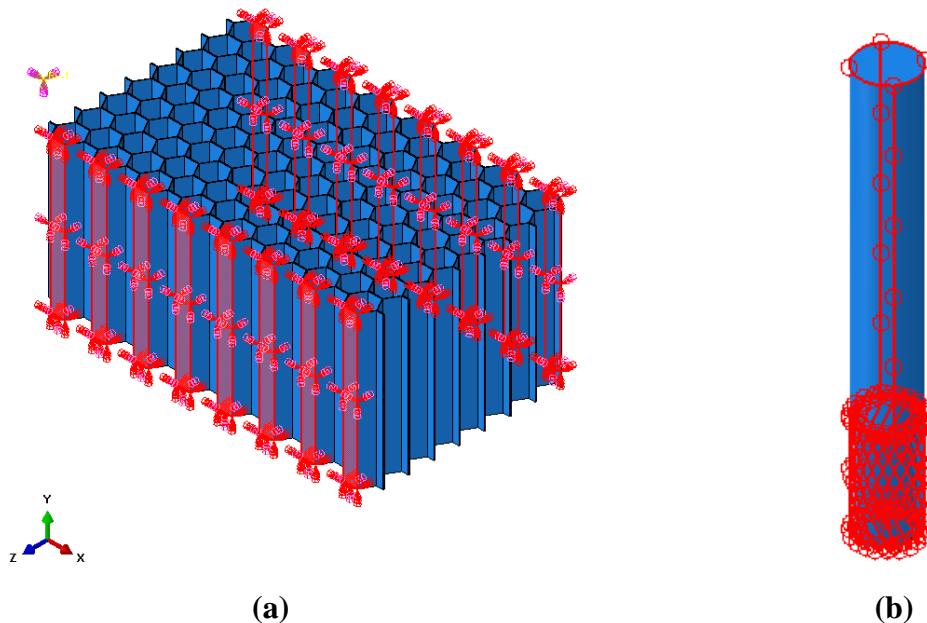


Figure 33 (a) Encastre Constraint for workpiece (b) Rigid Body for tool

The meshing was based on structured hexagonal elements. Hexagonal mesh properties refer to the characteristics and specifications of a mesh that is primarily composed of hexahedral (hex) elements. Hexahedral elements are three-dimensional finite elements with six faces, eight nodes, and twelve edges, which are shaped like a cube. These elements are commonly used for simulating solid structures due to their ability to accurately represent the behaviour of many engineering materials. The mesh is shown in Fig. 34. The results of the honeycomb core are depicted in Fig. 35.

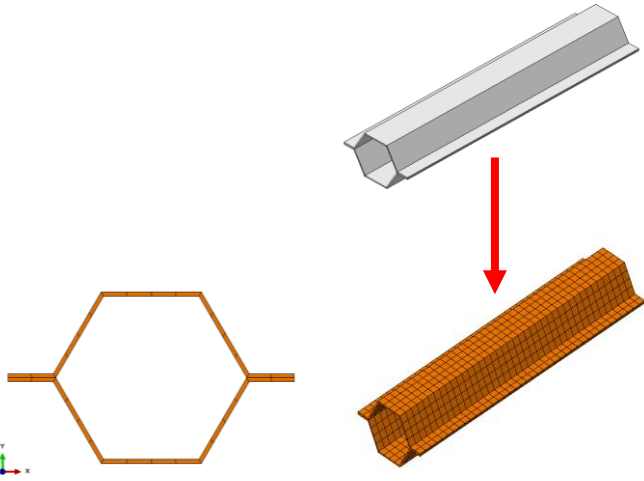


Figure 34 Meshing of Honeycomb Core

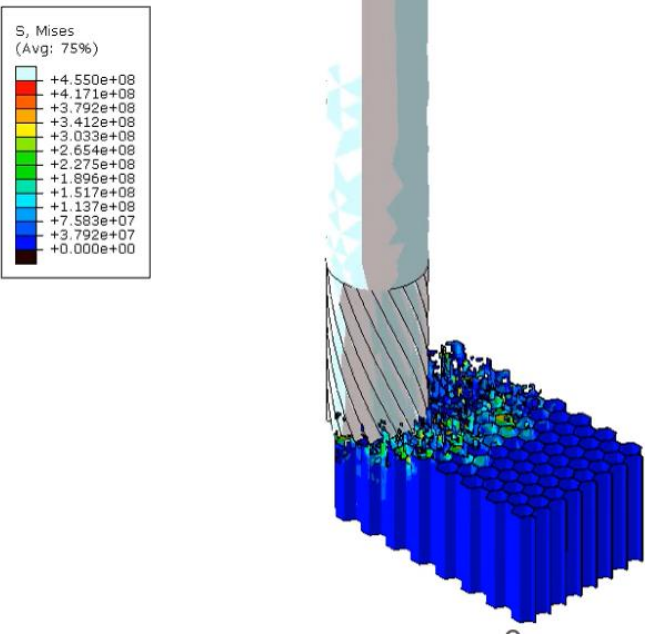


Figure 35 Simulation Results

Chapter 5: Conclusions and Recommendations

This chapter concludes the current dissertation by elaborating the main results and recommendations for future research in this particular topic of honeycomb core machining.

5.1 Conclusions

The current research was undertaken to optimize the machining process of Nomex Honeycomb cores. The machining is extensively used in the aerospace industry to make composite parts and assemblies which are heavily profiled and machining them becomes necessary. The machining process knowledge is required in detail to make perfect cutting of Nomex Honeycomb core to avoid the machining defects that have reportedly occurred during this process. The defects were of various kinds, including burr formation, tearing, delamination, and fraying. These defects can lead to the failure of subsequent sandwich structures after they have been manufactured using composite lay-up on honeycomb cores. The quality of machining is reportedly affected by the forces acting on the workpiece during machining and cutting efficiency. Both these parameters were taken together to optimize the machining process.

Taguchi Design of Experiments L9 array was used to design the experimental iterations based on the parameters which were finalized by literature review. These included spindle speed, feed rate and depth of cut. Subsequently, force dynamometer was used to measure the forces. For the integration of workpiece with dynamometer a special fixture plate was designed to clamp honeycomb core with the fixture plate. Subsequently, experiments were conducted, and forces were calculated. To measure cutting efficiency Keyence dimensional measurement system was utilized. The results were compiled and were analysed by data analytics.

Response tables from Taguchi were analysed to find out the most significant factor and it turned out to be feed rate in case of forces and depth of cut in case of cutting efficiency. Afterwards, ANOVA analysis was done and it indicates that the feed rate was the most significant factor with percentage contribution of 72% affecting cutting forces, whereas, depth of cut was most significant in case of cutting efficiency with percentage contribution of 85%. The significance of feed rate for cutting forces had a p-value of 0.01, followed by Spindle Speed 0.029 and Depth of Cut 0.247.

The depth of cut had a notable impact on cutting efficiency with a p-value of 0.023 followed by Feed Rate 0.217 and Spindle Speed 0.285.

Afterwards, multi-objective response optimization was done by using composite desirability function (DFA) and Grey Relational Analysis (GRA) Techniques. Composite Desirability was determined to be 86% indicating significance of optimization methodology. The results of Grey Relational Analysis (GRA) correlated with the DFA results and both techniques demonstrate similar optimal settings of response parameters. The optimal settings were found to be 6000 rpm of spindle speed, 100 mm/min feed rate and 15mm Depth of Cut.

Afterwards, ANOVA based prediction of parameters was found to be correct in comparison to the experimental validation results for the optimal settings and the error was within 5%. The percentage improvement in cutting forces was found out to be 47.8% as compared to the worst experimental run and cutting efficiency was improved by 11%.

The simulation of the process of machining was done using ABAQUS and it was revealed that extensive work is required to apply 3D Hashin Damage Criteria in VUMAT/UMAT. However, the simulation results built on Johnson Cook method was utilized to run simulations successfully.

5.2 Future Recommendations

This work has many dimensions for expansion and can form the basis of future research. Following vistas of exploration are recommended for future research works:

1. Evaluation of cutting efficiency and forces with additional types of tools and their configurations.
2. 5-axis machining process simulation based on the validated results of this research could be investigated for profiling of honeycomb cores.
3. Study of various other machining processes that could be carried out on HC Cores

4. 3D Hashin Criteria can be used to predict failure through simulation, however, it requires extensive coding in VUMAT/UMAT. One approach is to build an equivalent damage model based on a different damage already available in ABAQUS

5. Evaluation of machining defects with regards to the quality of composite structures can be evaluated to determine the level of accuracy required in machining to achieve best results for composite structures.

REFERENCES

- Aerospace Engineering and Operations Technician, Bureau of Labor Statistics, U.S. Department of Labor. (n.d.). *Honeycomb Structures*. www.bls.gov/ooh/architecture-and-engineering/aerospace-engineering-and-operations-technicians.htm#tab-2.
- Ahmad, S., Zhang, J., Feng, P., Yu, D., & Wu, Z. (2020). Experimental study on rotary ultrasonic machining (RUM) characteristics of Nomex honeycomb composites (NHCs) by circular knife cutting tools. *Journal of Manufacturing Processes*, 58(August), 524–535. <https://doi.org/10.1016/j.jmapro.2020.08.023>
- Chiang Foo, C., Boay Chai, G., & Keey Seah, L. (2006). *Mechanical properties of Nomex material and Nomex honeycomb structure*. <https://doi.org/10.1016/j.compstruct.2006.07.010>
- Davim, J. P., Reis, P., & António, C. C. (2004). A study on milling of glass fiber reinforced plastics manufactured by hand-lay up using statistical analysis (ANOVA). *Composite Structures*, 64(3–4), 493–500. <https://doi.org/10.1016/j.compstruct.2003.09.054>
- Girolamo, D., Chang, H. Y., & Yuan, F. G. (2018). Impact damage visualization in a honeycomb composite panel through laser inspection using zero-lag cross-correlation imaging condition. *Ultrasonics*, 87, 152–165. <https://doi.org/10.1016/j.ultras.2018.02.014>
- Haddad, M., Zitoune, R., Eyma, F., & Castanie, B. (2014). Study of the surface defects and dust generated during trimming of CFRP: Influence of tool geometry, machining parameters and cutting speed range. *Composites Part A: Applied Science and Manufacturing*, 66, 142–154. <https://doi.org/10.1016/j.compositesa.2014.07.005>
- Hashin, Z. (1980). *Fatigue failure criteria for unidirectional fiber composites*. <https://doi.org/AD-A088733>
- Heimbs, S. (2009a). FE-Simulation zur Bestimmung der mechanischen Eigenschaften. *Lightweight Design 2009* 2:3, 2(3), 52–57. <https://doi.org/10.1007/BF03223575>
- Heimbs, S. (2009b). Virtual testing of sandwich core structures using dynamic finite element simulations. *Computational Materials Science*, 45(2), 205–216. <https://doi.org/10.1016/j.commatsci.2008.09.017>
- HEXCEL. (2015). *Attributes and Properties guide to standard Hexcel honeycomb materials , properties. Honeycomb Composite*. (n.d.). Retrieved May 27, 2023, from <https://www.dupont.com/fabrics-fibers-and-nonwovens/honeycomb-composites.html>
- Hu, L. L., & Yu, T. X. (2010). Dynamic crushing strength of hexagonal honeycombs. *International Journal of Impact Engineering*, 37(5), 467–474. <https://doi.org/10.1016/J.IJIMPENG.2009.12.001>
- Jaafar, M., Atlati, S., Makich, H., Nouari, M., Moufki, A., & Julliere, B. (2017). A 3D FE Modeling of Machining Process of Nomex® Honeycomb Core: Influence of the Cell Structure Behaviour and Specific Tool Geometry. *Procedia CIRP*, 58, 505–510. <https://doi.org/10.1016/j.procir.2017.03.255>
- Jaafar, M., Makich, H., & Nouari, M. (2021). A new criterion to evaluate the machined surface quality of the Nomex® honeycomb materials. *Journal of Manufacturing Processes*, 69(August), 567–582. <https://doi.org/10.1016/j.jmapro.2021.07.062>
- Jaafar, M., Nouari, M., Makich, H., & Moufki, A. (2021). 3D numerical modeling and experimental validation of machining Nomex® honeycomb materials. *International Journal of Advanced Manufacturing Technology*,

- 115(9–10), 2853–2872. <https://doi.org/10.1007/s00170-021-07336-4>
- Jenarthanan, M. P., & Jeyapaul, R. (2018). Optimisation of machining parameters on milling of GFRP composites by desirability function analysis using Taguchi method. *International Journal of Engineering, Science and Technology*, 5(4), 22–36. <https://doi.org/10.4314/ijest.v5i4.3>
- Ju-Long, D. (1982). Control problems of grey systems. *Systems and Control Letters*, 1(5), 288–294. [https://doi.org/10.1016/S0167-6911\(82\)80025-X](https://doi.org/10.1016/S0167-6911(82)80025-X)
- Khan, M. S., Abdul-Latif, A., Kolor, S. S., Petru, M., & Tamin, M. N. (2021). Representative Cell Analysis for Damage-Based Failure Model of Polymer Hexagonal Honeycomb Structure under the Out-of-Plane Loadings. In *Polymers* (Vol. 13, Issue 1). <https://doi.org/10.3390/polym13010052>
- Ko, F. K., & Wu, G. W. (1998). Chapter 18 - Textile Preforming in: S. T. Peters (Ed.), *Handbook of Composites*. Chapman & Hall, 397–424.
- Li, C., Duan, C., & Chang, B. (2022). Instantaneous cutting force model considering the material structural characteristics and dynamic variations in the entry and exit angles during end milling of the aluminum honeycomb core. *Mechanical Systems and Signal Processing*, 181(June), 109456. <https://doi.org/10.1016/j.ymsp.2022.109456>
- Li, Z., & Ma, J. (2020). Experimental Study on Mechanical Properties of the Sandwich Composite Structure Reinforced by Basalt Fiber and Nomex Honeycomb. In *Materials* (Vol. 13, Issue 8). <https://doi.org/10.3390/ma13081870>
- Liu, L., Wang, H., & Guan, Z. (2015). Experimental and numerical study on the mechanical response of Nomex honeycomb core under transverse loading. *Composite Structures*, 121, 304–314. <https://doi.org/10.1016/j.compstruct.2014.11.034>
- Makich, H., Nouari, M., & Jaafar, M. (2022). Surface integrity quantification in machining of aluminum honeycomb structure. *Procedia CIRP*, 108(C), 693–697. <https://doi.org/10.1016/j.procir.2022.03.107>
- Medium Size Finishing Tools-CoreHoggers*. (n.d.). Retrieved May 30, 2023, from <https://www.corehog.com/products/finishing-core-tools-medium-corehoggers>
- Modi, K. P., & Bhavsar, S. N. (2023). Multi-response optimization of magnetic abrasive finishing process parameters on AISI H13 hot die steel using grey relational analysis. *Materials Today: Proceedings*, xxx, 1–7. <https://doi.org/10.1016/j.matpr.2023.01.381>
- Padhi, G. S., Sheno, R. A., Moy, S. S. J., & Hawkins, G. L. (1997). Progressive failure and ultimate collapse of laminated composite plates in bending. *Composite Structures*, 40(3–4), 277–291. [https://doi.org/10.1016/S0263-8223\(98\)00030-0](https://doi.org/10.1016/S0263-8223(98)00030-0)
- Qiu, K., Ming, W., Shen, L., An, Q., & Chen, M. (2017). Study on the cutting force in machining of aluminum honeycomb core material. *Composite Structures*, 164, 58–67. <https://doi.org/10.1016/j.compstruct.2016.12.060>
- Rion, J., Leterrier, Y., & Manson, J. A. E. (2008). Prediction of the adhesive fillet size for skin to honeycomb core bonding in ultra-light sandwich structures. *Composites Part A: Applied Science and Manufacturing*, 39(9), 1547–1555. <https://doi.org/10.1016/j.compositesa.2008.05.022>

- Roy, R., Nguyen, K. H., Park, Y. B., Kweon, J. H., & Choi, J. H. (2014). Testing and modeling of Nomex™ honeycomb sandwich Panels with bolt insert. *Composites Part B: Engineering*, *56*, 762–769. <https://doi.org/10.1016/j.compositesb.2013.09.006>
- Roy, R., Park, S. J., Kweon, J. H., & Choi, J. H. (2014). Characterization of Nomex honeycomb core constituent material mechanical properties. *Composite Structures*, *117*(1), 255–266. <https://doi.org/10.1016/j.compstruct.2014.06.033>
- Seemann, R., & Krause, D. (2017). Numerical modelling of Nomex honeycomb sandwich cores at meso-scale level. *Composite Structures*, *159*, 702–718. <https://doi.org/10.1016/j.compstruct.2016.09.071>
- Shivakumar, M. R., Hamritha, S., Shilpa, M., Mirunalini, & Gouda, K. S. (2020). Optimization of milling process parameters of aluminium alloy LM6 using response surface methodology. *Journal of Physics: Conference Series*, *1706*(1). <https://doi.org/10.1088/1742-6596/1706/1/012217>
- Song, Z., Luong, S., Whisler, D., & Kim, H. (2021). Honeycomb core failure mechanism of CFRP/Nomex sandwich panel under multi-angle impact of hail ice. *International Journal of Impact Engineering*, *150*(January), 103817. <https://doi.org/10.1016/j.ijimpeng.2021.103817>
- Sun, J., Dong, Z., Wang, X., Wang, Y., Qin, Y., & Kang, R. (2020). Simulation and experimental study of ultrasonic cutting for aluminum honeycomb by disc cutter. *Ultrasonics*, *103*, 106102. <https://doi.org/10.1016/J.ULTRAS.2020.106102>
- Vijayakumar, R., & Pannirselvam, N. (2022). Employing desirability function analysis for the multi-response optimisation of mild steel embossed plate shear connector using Taguchi technique. *Sustainable Energy Technologies and Assessments*, *54*(October), 102863. <https://doi.org/10.1016/j.seta.2022.102863>
- Wang, C. H., & Duong, C. N. (2016). Failure criteria. *Bonded Joints and Repairs to Composite Airframe Structures*, 21–45. <https://doi.org/10.1016/B978-0-12-417153-4.00002-5>
- Wang, X. M., & Zhang, L. C. (2003). An experimental investigation into the orthogonal cutting of unidirectional fibre reinforced plastics. *International Journal of Machine Tools and Manufacture*, *43*(10), 1015–1022. [https://doi.org/10.1016/S0890-6955\(03\)00090-7](https://doi.org/10.1016/S0890-6955(03)00090-7)
- Wang, Y., Gan, Y., Liu, H., Han, L., Wang, J., & Liu, K. (2020). Surface Quality Improvement in Machining an Aluminum Honeycomb by Ice Fixation. *Chinese Journal of Mechanical Engineering (English Edition)*, *33*(1), 1–8. <https://doi.org/10.1186/s10033-020-00439-1>
- Wang, Z., Qin, Q., Chen, S., Yu, X., Li, H., & Wang, T. J. (2017). Compressive crushing of novel aluminum hexagonal honeycombs with perforations: Experimental and numerical investigations. *International Journal of Solids and Structures*, *126–127*, 187–195. <https://doi.org/10.1016/J.IJSOLSTR.2017.08.005>
- Xu, Q., Bao, Y., Wang, Y. Q., & Gao, H. (2021). Investigation on damage reduction method by varying cutting angles in the cutting process of rectangular Nomex honeycomb core. *Journal of Manufacturing Processes*, *68*(PA), 1803–1813. <https://doi.org/10.1016/j.jmapro.2021.07.006>
- Zarrouk, T., Atlati, S., Salhi, M., & Nouari, M. (2020). *the Influence of Machining Conditions on the Milling Operations of Nomex Honeycomb Structure*. January, 1–11.
- Zarrouk, T., Nouari, M., & Makich, H. (2023). Simulated Study of the Machinability of the Nomex Honeycomb

- Structure. *Journal of Manufacturing and Materials Processing*, 7(1). <https://doi.org/10.3390/jmmp7010028>
- Zarrouk, T., Nouari, M., Salhi, J. E., Makich, H., Salhi, M., Atlati, S., & Salhi, N. (2022). Optimization of the milling process for aluminum honeycomb structures. *International Journal of Advanced Manufacturing Technology*, 119(7–8), 4733–4744. <https://doi.org/10.1007/s00170-021-08495-0>
- Zarrouk, T., Salhi, J. E., Atlati, S., Nouari, M., Salhi, M., & Salhi, N. (2021). Study on the behavior law when milling the material of the Nomex honeycomb core. *Materials Today: Proceedings*, 45, 7477–7485. <https://doi.org/10.1016/j.matpr.2021.02.110>
- Zarrouk, T., Salhi, J. E., Atlati, S., Nouari, M., Salhi, M., & Salhi, N. (2022). Modeling and numerical simulation of the chip formation process when machining Nomex. *Environmental Science and Pollution Research*, 29(1), 98–105. <https://doi.org/10.1007/s11356-021-13736-6>
- Zarrouk, T., Salhi, J. E., Nouari, M., Salhi, M., Atlati, S., Salhi, N., & Makich, H. (2021). Analysis of friction and cutting parameters when milling honeycomb composite structures. *Advances in Mechanical Engineering*, 13(7), 1–11. <https://doi.org/10.1177/16878140211034841>
- Zenia, S., Ben Ayed, L., Nouari, M., & Delamézière, A. (2015). An elastoplastic constitutive damage model to simulate the chip formation process and workpiece subsurface defects when machining CFRP composites. *Procedia CIRP*, 31, 100–105. <https://doi.org/10.1016/j.procir.2015.03.100>
- Zenkert, D. (1995). An introduction to sandwich construction. Engineering Materials Advisory Services. *Sheffield, UK*.
- Zinno, A., Prota, A., Di Maio, E., & Bakis, C. E. (2011). Experimental characterization of phenolic-impregnated honeycomb sandwich structures for transportation vehicles. *Composite Structures*, 93(11), 2910–2924. <https://doi.org/10.1016/j.compstruct.2011.05.012>

APPENDIX A

VISUAL RESULTS OF EXPERIMENTS

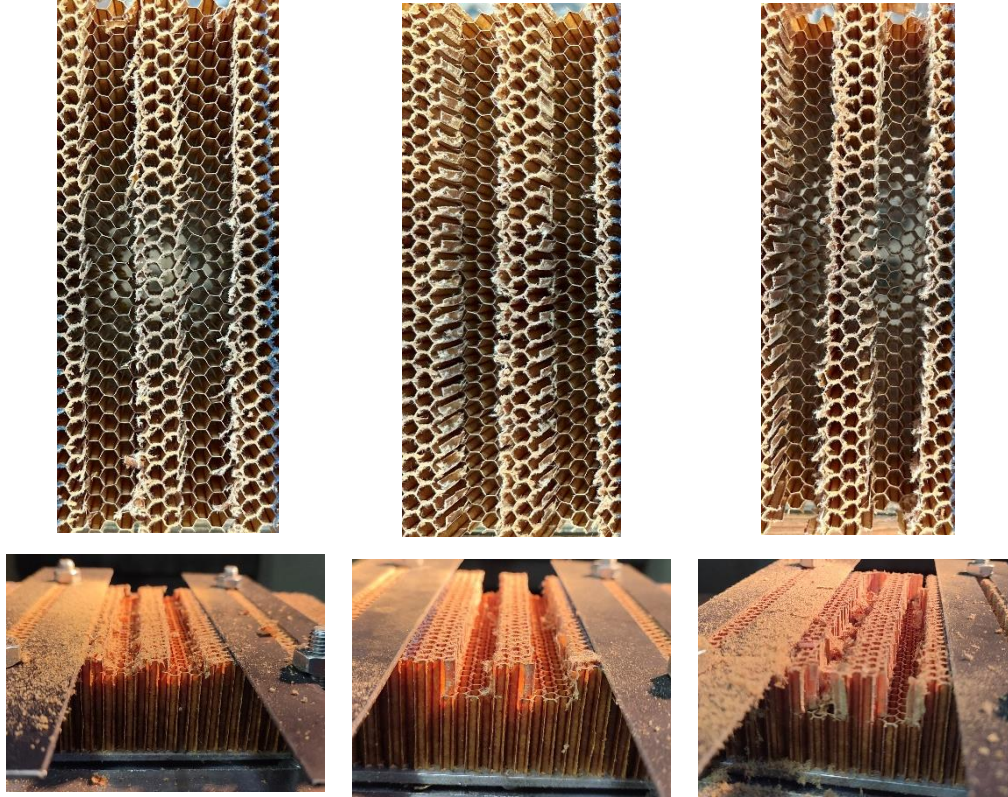


Figure 37 Experiment # 1, 2, 3

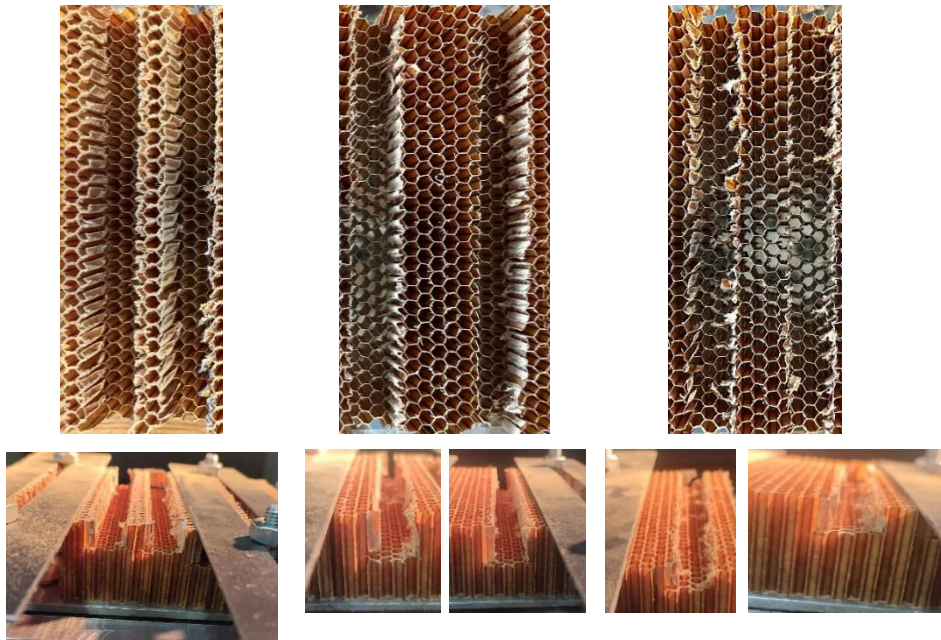


Figure 36 Experiment # 4, 5, 6

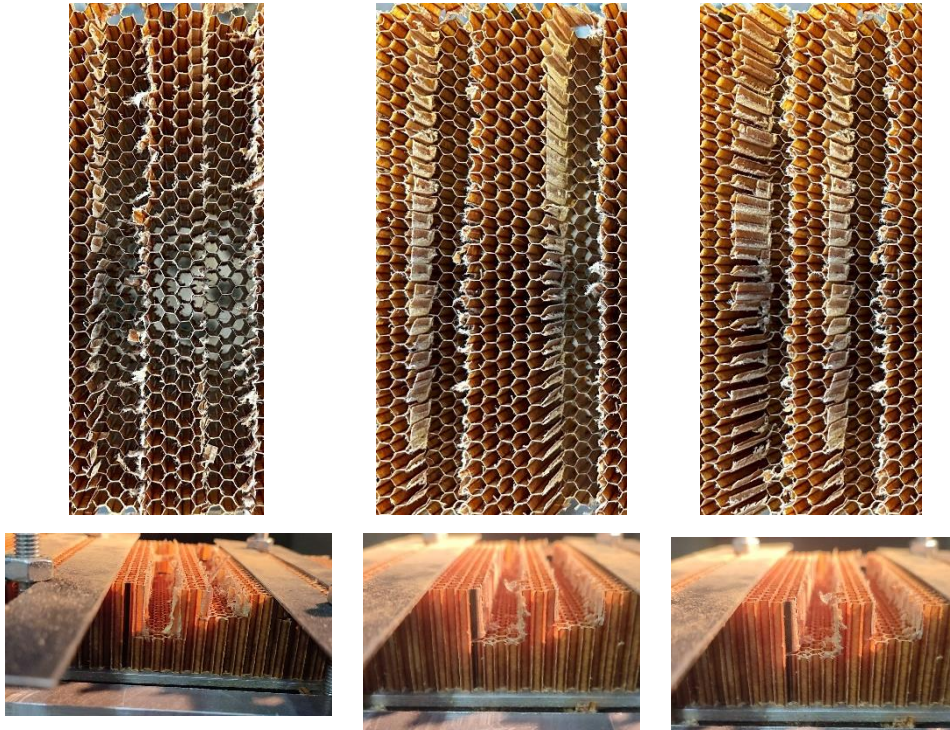
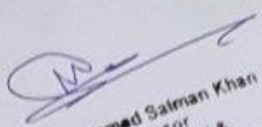


Figure 38 Experiment # 7, 8, 9

Hassan Thesis

ORIGINALITY REPORT


Dr. Muhammad Salman Khan
Assistant Professor
School of Mechanical &
Manufacturing Engineering
(SMME) NUST, Islamabad

5%

SIMILARITY INDEX

6%

INTERNET SOURCES

5%

PUBLICATIONS

3%

STUDENT PAPERS

PRIMARY SOURCES

1	hal.univ-lorraine.fr Internet Source	2%
2	www.coursehero.com Internet Source	2%
3	Submitted to Higher Education Commission Pakistan Student Paper	1%
4	Handbook of Composites, 1998. Publication	1%

Exclude quotes Off

Exclude bibliography On

Exclude matches < 1%